**GEORGIA DOT RESEARCH PROJECT 19-17**

**FINAL REPORT**

# ENHANCED NETWORK-LEVEL CURVE SAFETY ASSESSMENT AND MONITORING USING MOBILE DEVICES


**OFFICE OF PERFORMANCE-BASED MANAGEMENT AND RESEARCH**

**600 WEST PEACHTREE STREET NW**
**ATLANTA, GA 30308**

# TECHNICAL REPORT DOCUMENTATION PAGE

| | | | |
|---|---|---|---|
| 1. Report No.:<br>FHWA-GA-21-1917 | 2. Government Accession No.:<br>N/A | 3. Recipient's Catalog No.:<br>N/A | |
| 4. Title and Subtitle:<br>An Enhanced Network-Level Curve Safety Assessment and Monitoring Using Mobile Devices | | 5. Report Date:<br>July 2021<br>6. Performing Organization Code:<br>N/A | |
| 7. Author(s):<br>Yichang (James) Tsai, Ph.D., P.E. (https://orcid.org/0000-0002-6650-2279), Pingzhou Lucas Yu, Tianqi Liu, Zhongyu Yang, Ariel Steele. | | 8. Performing Organ. Report No.: 19-17 | |
| 9. Performing Organization Name and Address:<br>Georgia Institute of Technology<br>790 Atlantic Drive<br>Atlanta, GA 30332-0355<br>Email: james.tsai@ce.gatech.edu | | 10. Work Unit No.:<br>N/A<br>11. Contract or Grant No.:<br>PI# 0016839 | |
| 12. Sponsoring Agency Name and Address:<br>Georgia Department of Transportation<br>Office of Performance-Based Management and Research<br>600 West Peachtree St. NW<br>Atlanta, GA 30308 | | 13. Type of Report and Period Covered:<br>Final Report; July 2019 – July 2021<br>14. Sponsoring Agency Code:<br>N/A | |
| 15. Supplementary Notes:<br>Prepared in cooperation with the U.S. Department of Transportation, Federal Highway Administration. | | | |
| 16. Abstract:<br>A disproportionally high number of serious vehicle crashes (25% of fatal crashes) occur on horizontal curves, even though curves represent only a fraction of the roadway network (5% of highway miles) (FHWA, 2021; Atkinson et al., 2016). The in-service curve characteristics information, including curve radius, superelevation, and BBI angles, are extremely important for setting up adequate advisory speeds and for performing curve safety assessment and analysis. However, current transportation agencies' practices, using dedicated devices operated by designated engineers are labor-intensive, time-consuming, and costly. The objectives of this research project are 1) to develop an enhanced curve safety assessment method that uses low-cost mobile devices and new computation methods and 2) to critically assess the feasibility of the proposed method for network level curve safety condition assessment. The proposed method, using a new intra-agency, crowdsourced data collection and computational framework, leverages a) existing, low-cost mobile devices for collecting multiple runs of sensor data, including GPS data and IMU data, and b) agencies' existing vehicles and transportation engineers. The proposed data collection and computation framework consists of the following six modules: 1) mobile data collection, 2) mobile data registration and processing, 3) driving kinematics calculation, 4) curve geometry calculation, 5) advisory speed calculation, and 6) curve warning sign design. A refined superelevation computation method has been proposed in this study by revising path radius calculation using gyroscope data and GPS speeds, and refining a body roll calculation with a calibration procedure to estimate a vehicle's roll rate. The proposed method is validated using smartphone data collected from the NCAT test track with ground reference superelevation measurements. Results show that, using smartphones, the accuracy of superelevation computation can consistently achieve an RMSE of below 1.5 % slope at different speeds after using the calibration procedure to estimate the vehicle's roll rate; without roll rate estimation, the accuracy will continuously decrease with increasing speed, up to an RMSE of 3.2 % slope at high speed. A preliminary case study using multi-run smartphone data collected on Georgia State Route17 demonstrates the feasibility of the proposed method. | | | |
| 17. Key Words:<br>Ball Bank Indicator, Superelevation, Horizontal Curve Safety, Low-cost Mobile Device, Crowdsourcing | | 18. Distribution Statement:<br>No Restriction. | |
| 19. Security Classification (of this report): Unclassified | 20. Security classification (of this page): Unclassified | 21. Number of Pages: 98 | 22. Price:<br>Free |

**Form DOT 1700.7 (8-72)** Reproduction of completed page authorized.

GDOT Research Project 19-17

Final Report

# ENHANCED NETWORK-LEVEL CURVE SAFETY ASSESSMENT AND MONITORING USING MOBILE DEVICES

By
Yichang (James) Tsai, Ph.D., P.E.
Professor of Civil and Environmental Engineering

Pingzhou Lucas Yu
Graduate Research Assistant

Tianqi Liu
Graduate Research Assistant

Zhongyu Yang
Graduate Research Assistant

Ariel Steele
Graduate Research Assistant

Georgia Tech Research Corporation

Contract with
Georgia Department of Transportation

In cooperation with
U.S. Department of Transportation
Federal Highway Administration

July 2021

# SI* (MODERN METRIC) CONVERSION FACTORS

## APPROXIMATE CONVERSIONS TO SI UNITS

| Symbol | When You Know | Multiply By | To Find | Symbol |
|---|---|---|---|---|
| | | **LENGTH** | | |
| in | inches | 25.4 | millimeters | mm |
| ft | feet | 0.305 | meters | m |
| yd | yards | 0.914 | meters | m |
| mi | miles | 1.61 | kilometers | km |
| | | **AREA** | | |
| $in^2$ | square inches | 645.2 | square millimeters | $mm^2$ |
| $ft^2$ | square feet | 0.093 | square meters | $m^2$ |
| $yd^2$ | square yard | 0.836 | square meters | $m^2$ |
| ac | acres | 0.405 | hectares | ha |
| $mi^2$ | square miles | 2.59 | square kilometers | $km^2$ |
| | | **VOLUME** | | |
| fl oz | fluid ounces | 29.57 | milliliters | mL |
| gal | gallons | 3.785 | liters | L |
| $ft^3$ | cubic feet | 0.028 | cubic meters | $m^3$ |
| $yd^3$ | cubic yards | 0.765 | cubic meters | $m^3$ |
| | NOTE: volumes greater than 1000 L shall be shown in $m^3$ | | | |
| | | **MASS** | | |
| oz | ounces | 28.35 | grams | g |
| lb | pounds | 0.454 | kilograms | kg |
| T | short tons (2000 lb) | 0.907 | megagrams (or "metric ton") | Mg (or "t") |
| | | **TEMPERATURE (exact degrees)** | | |
| $^oF$ | Fahrenheit | 5 (F-32)/9<br>or (F-32)/1.8 | Celsius | $^oC$ |
| | | **ILLUMINATION** | | |
| fc | foot-candles | 10.76 | lux | lx |
| fl | foot-Lamberts | 3.426 | candela/$m^2$ | $cd/m^2$ |
| | | **FORCE and PRESSURE or STRESS** | | |
| lbf | poundforce | 4.45 | newtons | N |
| $lbf/in^2$ | poundforce per square inch | 6.89 | kilopascals | kPa |

## APPROXIMATE CONVERSIONS FROM SI UNITS

| Symbol | When You Know | Multiply By | To Find | Symbol |
|---|---|---|---|---|
| | | **LENGTH** | | |
| mm | millimeters | 0.039 | inches | in |
| m | meters | 3.28 | feet | ft |
| m | meters | 1.09 | yards | yd |
| km | kilometers | 0.621 | miles | mi |
| | | **AREA** | | |
| $mm^2$ | square millimeters | 0.0016 | square inches | $in^2$ |
| $m^2$ | square meters | 10.764 | square feet | $ft^2$ |
| $m^2$ | square meters | 1.195 | square yards | $yd^2$ |
| ha | hectares | 2.47 | acres | ac |
| $km^2$ | square kilometers | 0.386 | square miles | $mi^2$ |
| | | **VOLUME** | | |
| mL | milliliters | 0.034 | fluid ounces | fl oz |
| L | liters | 0.264 | gallons | gal |
| $m^3$ | cubic meters | 35.314 | cubic feet | $ft^3$ |
| $m^3$ | cubic meters | 1.307 | cubic yards | $yd^3$ |
| | | **MASS** | | |
| g | grams | 0.035 | ounces | oz |
| kg | kilograms | 2.202 | pounds | lb |
| Mg (or "t") | megagrams (or "metric ton") | 1.103 | short tons (2000 lb) | T |
| | | **TEMPERATURE (exact degrees)** | | |
| $^oC$ | Celsius | 1.8C+32 | Fahrenheit | $^oF$ |
| | | **ILLUMINATION** | | |
| lx | lux | 0.0929 | foot-candles | fc |
| $cd/m^2$ | candela/$m^2$ | 0.2919 | foot-Lamberts | fl |
| | | **FORCE and PRESSURE or STRESS** | | |
| N | newtons | 0.225 | poundforce | lbf |
| kPa | kilopascals | 0.145 | poundforce per square inch | $lbf/in^2$ |

* SI is the symbol for the International System of Units. Appropriate rounding should be made to comply with Section 4 of ASTM E380. (Revised March 2003)

# TABLE OF CONTENTS

# LIST OF FIGURES

# LIST OF TABLES

# LIST OF ABBREVIATIONS

| | |
|---|---|
| AASHTO | American Association of State Highway and Transportation Officials |
| BBI | Ball Back Indicator |
| CARS | Curve Advisory Reporting System |
| CSAM | Curve Safety Assessment and Monitoring |
| CMF | Crash Modification Factors |
| DOT | Department of Transportation |
| DEG | Degree |
| FHWA | Federal Highway Administration |
| GPS | Global Positioning System |
| GTSV | Georgia Tech Sensing Vehicle |
| IMU | Inertial Measurement Unit |
| MUTCD | Manual on Uniform Traffic Control Devices |
| NCAT | National Center for Asphalt Technology |
| NCHRP | National Cooperative Highway Research Program |
| PC | Point of Curve |
| PT | Point of Tangent |
| RMSE | Root Mean Squared Error |
| SR | State Route |
| TRAMS | Texas Roadway Analysis and Measurement Software |
| TTI | Texas A&M Transportation Institute |

# EXECUTIVE SUMMARY

A disproportionally high number of serious vehicle crashes (25% of fatal crashes) occur on horizontal curves, even though curves represent only a fraction of the roadway network (5% of highway miles) (FHWA, 2021; Atkinson et al., 2016). This is a high-priority problem that has great interest among transportation agencies throughout the nation because the ultimate goal is to reduce serious vehicle crashes on curves. The problem is complicated because, based on our communication with state DOTs' engineers, the in-service curve characteristics, including superelevation, may change over time because of new pavement resurfacings. Therefore, understanding in-service curve characteristics is vital to improving the safety of curves. The in-service curve characteristics, including curve radius, superelevation, and BBI angles, are vitally important for setting up adequate curve advisory speeds and for performing curve safety assessment and analysis. However, current transportation agencies' practices use dedicated devices operated by designated engineers to collect curve characteristics information at network-level for curve safety condition assessment. The practices are typically labor-intensive, time-consuming, and costly.

With the advancement of sensor technologies, low-cost mobile devices (such as smartphones, tablet PCs, GoPro cameras, etc.) are capable of collecting GPS data, IMU data (accelerometer, magnetometer, and gyroscope data), and high-resolution roadway video log images. These sensor data can be used to compute curve characteristics information for network level curve safety assessment. There is an urgent need to develop an enhanced method to collect in-service curve characteristics in support of network level curve safety assessment, analysis, and improvement. The objectives of this research project are to develop an enhanced curve safety

assessment method that uses low-cost mobile devices and new proposed computation methods and to critically assess the feasibility of the proposed method for network level curve safety condition assessment.

The proposed method, using a new intra-agency, crowdsourced data collection and computational framework, leverages a) existing, low-cost mobile devices, (e.g., smartphones, tablet PCs, GoPro cameras, etc.) to collect multiple runs of sensor data, including GPS data and IMU data, and b) agencies' existing vehicles and transportation engineers (who can collect data while simultaneously performing other tasks). The proposed data collection and computation framework consists of six modules: 1) mobile data collection, 2) mobile data registration and processing, 3) driving kinematics calculation, 4) curve geometry calculation, 5) advisory speed calculation, and 6) curve warning sign design.

Superelevation is one of the important curve characteristics for setting up advisory speed limits and for curve safety analysis. Leveraging the concept in our previous research that aimed to estimate roadway superelevation using data collected by mobile devices, a refined method is proposed in this study. A refined superelevation computation method revises path radius calculation using gyroscope and GPS speeds, and it revises body roll calculation using a proposed calibration procedure to estimate vehicle roll rate and use the lateral acceleration experienced by a vehicle to calculate body roll. The proposed calibration can be done by collecting mobile data on curves with known superelevation or collecting multiple runs of data on the same curve at different speeds, without the need to manually measure true superelevation. The following are the conclusions for this research project.

1) A method using low-cost mobile devices and a new intra-agency, crowdsourced data collection and computational framework, has been developed to assist network-level

curve characteristics and safety condition assessment. The proposed data collection and computational framework consists of six modules: 1) mobile data collection, 2) mobile data registration and processing, 3) driving kinematics calculation, 4) curve geometry calculation, 5) advisory speed calculation, and 6) curve warning sign design. Key data items computed using the proposed method include BBI angles, curve radius, superelevation, and advisory speed.

2) The proposed method uses the vehicle's body roll that calculated from vehicle's roll rate for more accurate superelevation calculations. In addition, two calibration procedures were proposed to estimate the vehicle's roll rate.

3) A data collection application "All Gather" was built for Android smartphones. "AllGather" is an advanced dashcam-like application that collects a driving video log, GPS data, IMU data, and driving speed.

4) The proposed method has been validated using the data collected on 1.7 miles of the NCAT test track to evaluate the feasibility of using the proposed method to compute curve safety assessment-related data items using the data collected from mobile devices. Results show that the proposed method can achieve accurate results for computing superelevation, curve radius, BBI angle, and curve advisory speed.

    a) Using typical smartphones for data collection, the results of superelevation, without calibration to compensate for vehicle body roll, the superelevation measurement the accuracy continuously decrease with increasing speed, up to an RMSE of 3.2 % slope at high speed, which results in a 3 MPH difference in the determined advisory speed. With calibration using the proposed method, the superelevation results from smartphones can consistently achieve an RMSE of 1.4 – 1.5 % slope at different data collection speed, and the advisory speed result is about 1 MPH off from the advisory determined from the manually measured superelevation.

    b) The proposed method recommends the use of the curve centerline for curve radius estimation. A validation test shows that with a good quality centerline, the estimated curve radius is very close to the curve radius from the curve design drawings.

c) A sensitivity study conducted reveals that, since the advisory speed typically rounds down to the nearest 5 MPH, accuracy level of the data items computed will result in the determined advisory speed to be within the 5 MPH range of true advisory speed of the curve.

5) A preliminary case study using the proposed method and smartphone data collected on five curves with 5 runs of data collection on Georgia State Route 17 demonstrates it is feasible to compute curve characteristics information using typical smartphones. Using five curves with five runs of data collected in each driving direction, the results demonstrate the proposed method shows very little variability; in most cases, the five data collection runs resulted in the same advisory speed (after rounding down to the nearest 5 MPH), and in other cases, four out of five runs had the same advisory speed. This suggests the advisory speed obtained from the proposed method is highly repeatable. If using the variability between multiple runs of data collection as an indication of the confidence level of the data, this would suggest the results computed from the proposed method have a high confidence level.

The proposed method has been developed, and the preliminary study has shown the outcomes are promising. The following are the recommendations for the future work:

1) It is recommended to further evaluate and refine the proposed method, including the developed data collection application and computation method for implementation, by performing a pilot study to collect the data collected on roadways with diverse conditions (curve type, geometry, radius, etc.) and using state DOT-owned vehicles. It is recommended to compare the outcomes with the commonly used method using RIEKER devices.

2) It is recommended to explore the implementation of the proposed method in state DOTs' business operation of network-level curve safety assessment and analysis, and the establishment of advisory speeds on curves.

3) It is recommended to include local transportation agencies (counties and cities) in the pilot study because local transportation agencies have limited resources and the proposed

method would be very helpful to them (because of using low-cost devices) to improve their roadway safety assessment.

4) It is recommended to further evaluate the cost, performance, and practicality of other types of mobile devices for data collection.

5) It is recommended the proposed calibration method for estimating vehicle's roll rate be further researched using the mechanically measured roll rate as ground reference; also, further study should be performed to enhance the accuracy of the proposed estimation method and study the impact of estimation errors.

# CHAPTER 1. INTRODUCTION

A disproportionally high number of serious vehicle crashes (25% of fatal crashes) occur on horizontal curves, even though curves represent only a fraction of the roadway network (5% of highway miles) (FHWA, 2021; Atkinson et al., 2016). When the friction is insufficient to compensate for the lateral force experienced by a vehicle being driven on a curve, the vehicle will slide and run off the road (ROR). This is a high priority problem that has the great interest among transportation agencies throughout the nation because the ultimate goal is to reduce serious vehicle crashes on curves. The problem is complicated because, based on our communication with state DOTs' engineers, the in-service curve characteristics, including superelevation, may change over time because of new pavement resurfacings. Therefore, understanding in-service curve characteristics is vital to improving the safety of curves. The in-service curve characteristics, including curve radius, superelevation, and BBI angles, are vitally important for setting up adequate curve advisory speeds and for performing curve safety assessment and analysis. A BBI measurement is one of the important curve safety indicators specified by the MUTCD (2009); it is a combined indicator that includes curvature, superelevation, side friction condition, and driving speed.

However, acquiring this detailed level roadway characteristics information on in-service curves at the network level is very difficult for transportation agencies. For example, state DOTs, like the Georgia Department of Transportation (GDOT) use an electronic device (manufactured by Rieker) to collect BBI measurements in the field. For the curves to be assessed, GDOT engineers make more than two runs on each curve at incremental speeds and measure the BBI in each run to determine a curve's adequate advisory speed. This operation typically requires two workers

(one drives a vehicle while another records BBI) and is labor-intensive, time-consuming, and costly. Once a representative BBI value, along with an adequate advisory speed for each curve, has been determined, countermeasures (such as setting up an advisory speed at the beginning of the curve or applying a High Friction Surface Treatment (HFST) or some other treatment) can be applied based on an analysis of the potential safety improvement, completion of a benefit-cost ratio analysis, and determination of funding availability. In summary, current transportation agencies' practices use dedicated devices operated by designated engineers to collect curve characteristics information at network-level for curve safety condition assessment. The practices are typically labor-intensive, time-consuming, and costly.

Because the current practices and methods are time-consuming, labor-intensive, and costly, it typically takes one to two years to complete the curve safety assessment of 100% of their state-maintained roadways. For local transportation agencies (counties and cities) that have limited resources, the process of completing a network curve safety assessment can take longer. Thus, roadway curve sections that need safety improvement(s) are often not identified until accidents occur. Because of long intervals between curve safety assessments, it is difficult for DOTs to take proactive actions in terms of identifying problems or making timely curve safety improvements. The constraints of current practices and methods significantly hinder transportation agencies' capabilities to reduce the disproportionally high number of fatalities on curves. The problem of current practices significantly hinders transportation agencies' abilities to proactively apply safety improvements and reduce the number of crashes on roadway curves. Thus, there is an urgent need to develop enhanced methods that enable transportation agencies to perform network-level curve safety assessment in a timely, cost-effective, and safe manner. Because transportation agencies' funds/budgets are often limited and must be used wisely, an innovative

and cost-effective method that enables transportation agencies to do more with less is required.

With the advancement of sensor technologies, low-cost mobile devices (such as smartphones, tablet PCs, GoPro cameras, etc.) that usually integrate various sensors (such as GPS sensors, accelerometers, magnetometer, and gyroscopes) are available to collect sensor data and vehicle's kinematic parameters, such as vehicle speed, lateral acceleration, rolling angle, etc. These sensor data and vehicle's kinematic parameters can be used to compute curve characteristics information, including radius, superelevation, and BBI values for network level curve safety assessment.

The objectives of this research project are 1) to develop an enhanced curve safety assessment method that uses low-cost mobile devices and new proposed computation methods and 2) to critically assess the feasibility of the proposed method for network level curve safety condition assessment. The project will use intra-agency, crowdsourced, low-cost mobile devices and multi-run data analysis to identify, in a timely manner, problematic roadway curves that need safety improvement. The research project's overall objective is to reduce the current disproportionally high number of fatalities on roadway curves. The use of intra-agency, crowdsourced, low-cost mobile devices to collect sensor data on the roadway while engineers are performing other tasks can reduce engineers' time on the road and minimizes their exposure to hazardous curve sections.

Figure 1 illustrates the proposed methodology for timely curve safety assessment and improvement using low-cost mobile devices. As is currently done in Uber vehicles, low-cost devices, like smartphones, can be installed in state DOT vehicles. This method establishes a new intra-agency, crowdsourced data collection and computation framework by leveraging agencies' existing vehicles and transportation engineers. The framework uses low-cost mobile devices (e.g., smartphones and/or tablet PCs) for collecting data (including GPS data, accelerations,

gyroscope data, and image data) from multiple runs; using the framework, transportation engineers can collect data while performing other tasks.

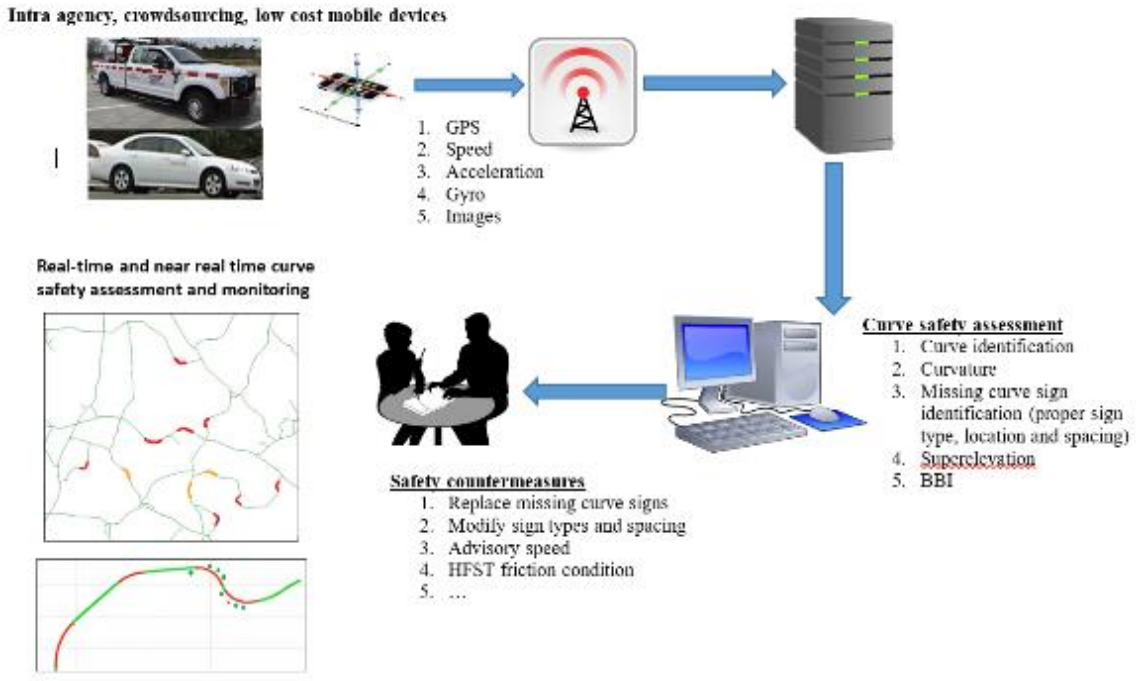


**Figure 1. Diagram. The proposed low-cost smartphone-based methodology for an accelerated curve safety assessment and improvement.**

As indicated, it is difficult for transportation agencies to take proactive action to make curve safety improvements in a timely manner because of the long interval between curve safety inspections (they are usually accomplished annually or bi-annually). The proposed methodology provides a low-cost means for transportation agencies to perform a preliminary network-level curve safety assessment screening on a daily or weekly schedule. Once roadway sections in need of curve safety improvement are identified, a detailed curve safety assessment can be conducted on the identified targeted sections. This enables transportation agencies to focus their time and attention on roadway curve sections that need improvement, not those that do not need improvement. This proactive and focused attention, done on a daily, weekly, or monthly basis

rather than an annual or biannual basis, will vastly improve the quality and timeliness of curve safety inspection and proactive improvements. The proposed methodology is aimed at enhancing the current network-level curve safety assessment method, which is costly, labor-intensive, time-consuming, and often dangerous. The proposed methodology provides a means for transportation agencies to proactively reduce fatalities in the most cost-effective and timeliest manner.

To optimize the data collection effort, the proposed methodology creatively utilizes intra-agency, crowdsourced, low-cost mobile devices. With the proposed method, roadway data can be collected using an agency's vehicles while its personnel are conducting other day-to-day operations. In this way, it is expected that the survey frequency can be increased from annually to, at least, weekly. Because an agency's vehicles traverse the same roads many times, multiple runs of data can be collected from different drivers at different times for a single curve section; the data can then be analyzed to eliminate biases that occur when data is collected only on a single run. Crowdsourcing data collected from the fleet and employees in a single transportation agency, i.e., intra-agency, can ensure data quality.

To the best of our knowledge, there are, currently, no crowdsourced, low-cost mobile applications that can productively and cost-effectively collect and analyze data (gathered from multiple runs by different drivers) for assessing roadway curve safety at the network level or that can perform BBI computation, super-elevation computation, and advisory speed determination**.** The proposed method, using a new intra-agency, crowdsourced data collection and computational framework, leverages a) existing, low-cost mobile devices, (e.g., smartphones, tablet PCs, GoPro cameras, etc.) to collect multiple runs of sensor data, including GPS data and IMU data, and b) agencies' existing vehicles and transportation engineers (who can collect data while simultaneously performing other tasks). The proposed data collection and computation

framework consists of six modules: 1) mobile data collection, 2) mobile data registration and processing, 3) driving kinematics calculation, 4) curve geometry calculation, 5) advisory speed calculation, and 6) curve warning sign design. The detailed data collection and computation framework is presented in Chapter 3.

## RESEARCH OBJECTIVES AND SCOPE

The objectives of this research project are 1) to develop an enhanced curve safety assessment method that uses low-cost mobile devices and new proposed computation methods and 2) to critically assess the feasibility of the proposed method for network level curve safety condition assessment. This research critically assesses the feasibility of using low-cost mobile devices to compute BBI, computing super-elevation, and determining accurately and reliably the adequate advisory speed. In addition, the refined superelevation computation algorithms using smart phone data, with a new calibration procedure, taking into account vehicle body roll, must be developed and validated so they can be used with confidence on different vehicles and under more general field conditions. The following are the major tasks:

1) Review existing regulations and current practices on network-level curve safety assessment, analysis, and management.
2) Develop an enhanced method using low-cost mobile devices with a proposed data collection and computation framework.
3) Propose the network-level smartphone-based ball-bank indicator (BBI) and curve superelevation computation method with a new calibration procedure, taking into account body roll to improve the accuracy of superelevation computation.
4) Develop temporal and spatial inter-device data referencing and registration methods.
5) Validate the proposed method, using the data collected on 1.7 miles of the Nation Center Asphalt Technology (NCAT) test track.
6) Summarize research findings.

## REPORT ORGANIZATION

This research project report is organized as follows. Chapter 1 presents the background, research needs, and research objectives and proposed tasks. Chapter 2 presents a literature review on existing regulations and current practices on network-level curve safety assessment, analysis, and management, and the research needs. Chapter 3 presents the proposed method with a data collection and computation framework for curve safety-related elements using mobile devices. Chapter 4 presents validation of the proposed method using data collected on 1.7 miles of the NCAT test track in Alabama with ground reference superelevation measurements in the field. Chapter 5 presents a preliminary case study on Georgia State Route 17 (SR 17) to demonstrate the use of the proposed method, using typical smartphones/mobile devices. Chapter 6 presents findings, conclusions, and recommendations for future work.

# CHAPTER 2. LITERATURE REVIEW ON REQUIRED CURVE & CURVE SIGN DESIGNS AND THEIR NETWORK LEVEL SAFETY ASSESSMENT

This chapter reviews the required curve and curve sign designs, presents the current practices and methods with a special focus on superelevation computation, and summarizes the technical challenges and needs for assessment improvement. The required curve geometric design and curve sign designs include designing the supply (e.g., superelevation, curve radius, and side friction) for meeting the demand (e.g. the advisory speed) specified in the AASHTO Green Book (AASHTO, 2011); setting up advisory speeds on curves and placing the required types of warning signs on curves, ensuring signs are placed at the required spacing and locations based on CRC and speed differentials between the posted speed and the advisory speed specified in the MUTCD (FHWA, 2009); assessing curve sign condition; and ensuring the required sight distance is correct as specified by the MUTCD. The curve roadway characteristics (CRC) information includes the detailed level curve information (e.g., radius, point of curve and point of tangent, and deviation angle), superelevation, and Ball Bank Indicator (BBI) and are often required to support network-level curve safety assessment, analysis, and improvement.

## REQUIRED SPECIFICATION FOR CURVE SAFETY MANAGEMENT

This section presents the required specifications for curve and curve sign designs; it also presents the practices and methods used for network-level curve safety assessment with a special focus on superelevation computation. In our study, we have focused on discussing regulations for curve and curve sign designs, curve sign condition assessment, and network level curve safety assessment of in-service curves. There are still other curve safety-related roadway elements, including sight distance, guardrail, etc., that are not included in our literature review. In this

chapter, we present the required curve geometry, including superelevation, curve radius and side friction for meeting the expected advisory speed, the required curve roadway characteristics for curve sign installation, and the requirements for sign condition assessment. Based on curve and curve sign design regulations, curve roadway characteristics (CRC) to be evaluated at the network level to ensure roadway safety can then be identified. As this CRC information is related to roadway safety, which is very important for transportation agencies to properly manage their roadways; it is essential to identify any deficiencies in a timely manner. In each subsection, the current methods to collect data and to perform design and assessment are also discussed. Finally, the challenges and needs for improvement are summarized.

**Geometric Design of Horizontal Curves**

Curve geometry design requirements can be found in the AASHTO Green Book (AASHTO, 2011). The main concept is to design the roadway geometry (e.g., superelevation, curve radius, and side friction) to meet the demand of the expected driving speed on a curve. The curve radius, superelevation, and friction are designed based on the design curve driving speed in the curve design stage. In our project, we assume we know curve radius, superelevation, and roadway side friction. Equation (1) illustrates the relationship between the expected driving speed on a curve, superelevation, curve radius, and side friction.

$$V^2 = 15(0.01e + f) * R \quad (1)$$

where $R$ is the radius (ft), $V$ is the vehicle speed (mph), $e$ is the average super-elevation, and $f$ is the side friction factor.

Once the curves have been built and are in service, the actual CRC information, including

superelevation, curve radius, and BBI, is often not available. This is because the as-built roadway characteristics information is typically different from the designed CRC information. In addition, the CRC information, like superelevation, changes with new pavement resurfacing. Based on our discussion with GDOT District engineers, the superelevation often changes with new pavement resurfacing, and sometimes, insufficient superelevation sections have caused accidents. In addition, due to the changes of curve design standards over time, substandard curves will need to be identified and corrected to ensure the safety of curves. Therefore, network-level curve safety assessment on in-service curves is very critical. However, current network-level curve safety assessment methods used on in-service curves are time-consuming, labor-intensive, and costly. Our research focuses on enhancing the current network-level curve safety assessment on in-service curves.

**Curve Warning Sign Design**

Curve sign design is required based on the MUTCD to ensure roadway safety (FHWA, 2009). The MUTCD, which has been administered by FHWA since 1971, is a compilation of national standards for all traffic control devices, including road markings, highway signs, and traffic signals. It is updated periodically to accommodate the nation's changing transportation needs and to address new safety technologies, traffic control tools, and traffic management techniques**.** In terms of curve safety, two things are critical for transportation agencies to determine: the curve advisory speed limit and the types, spacing, and locations of the curve signs that need to be placed. To determine the curve advisory speed and the placement of the curve warning signs, transportation agencies should follow the MUTCD guidelines, which contain information regarding the determination of curve advisory speeds and curve sign locations. The following tables from the MUTCD (2009 version) show that the advance placement distance of the curve

warning sign is dependent on the posted and advisory speed differentials, and the chevron sign intervals is decided by the advisory speed and the curve radius.

**Table 2C-4. Guidelines for Advance Placement of Warning Signs**

| Posted or 85th-Percentile Speed | Advance Placement Distance[1] | | | | | | | | |
|---|---|---|---|---|---|---|---|---|---|
| | Condition A: Speed reduction and lane changing in heavy traffic[2] | Condition B: Deceleration to the listed advisory speed (mph) for the condition | | | | | | | |
| | | 0[3] | 10[4] | 20[4] | 30[4] | 40[4] | 50[4] | 60[4] | 70[4] |
| 20 mph | 225 ft | 100 ft[6] | N/A[5] | – | – | – | – | – | – |
| 25 mph | 325 ft | 100 ft[6] | N/A[5] | N/A[5] | – | – | – | – | – |
| 30 mph | 460 ft | 100 ft[6] | N/A[5] | N/A[5] | – | – | – | – | – |
| 35 mph | 565 ft | 100 ft[6] | N/A[5] | N/A[5] | N/A[5] | – | – | – | – |
| 40 mph | 670 ft | 125 ft | 100 ft[6] | 100 ft[6] | N/A[5] | – | – | – | – |
| 45 mph | 775 ft | 175 ft | 125 ft | 100 ft[6] | 100 ft[6] | N/A[5] | – | – | – |
| 50 mph | 885 ft | 250 ft | 200 ft | 175 ft | 125 ft | 100 ft[6] | – | – | – |
| 55 mph | 990 ft | 325 ft | 275 ft | 225 ft | 200 ft | 125 ft | N/A[5] | – | – |
| 60 mph | 1,100 ft | 400 ft | 350 ft | 325 ft | 275 ft | 200 ft | 100 ft[6] | – | – |
| 65 mph | 1,200 ft | 475 ft | 450 ft | 400 ft | 350 ft | 275 ft | 200 ft | 100 ft[6] | – |
| 70 mph | 1,250 ft | 550 ft | 525 ft | 500 ft | 450 ft | 375 ft | 275 ft | 150 ft | – |
| 75 mph | 1,350 ft | 650 ft | 625 ft | 600 ft | 550 ft | 475 ft | 375 ft | 250 ft | 100 ft[6] |

**Table 2C-6. Typical Spacing of Chevron Alignment Signs on Horizontal Curves**

| Advisory Speed | Curve Radius | Sign Spacing |
|---|---|---|
| 15 mph or less | Less than 200 feet | 40 feet |
| 20 to 30 mph | 200 to 400 feet | 80 feet |
| 35 to 45 mph | 401 to 700 feet | 120 feet |
| 50 to 60 mph | 701 to 1,250 feet | 160 feet |
| More than 60 mph | More than 1,250 feet | 200 feet |

**Table 2C-5. Horizontal Alignment Sign Selection**

| Type of Horizontal Alignment Sign | Difference Between Speed Limit and Advisory Speed | | | | |
|---|---|---|---|---|---|
| | 5 mph | 10 mph | 15 mph | 20 mph | 25 mph or more |
| Turn (W1-1), Curve (W1-2), Reverse Turn (W1-3), Reverse Curve (W1-4), Winding Road (W1-5), and Combination Horizontal Alignment/Intersection (W1-10) (see Section 2C.07 to determine which sign to use) | Recommended | Required | Required | Required | Required |
| Advisory Speed Plaque (W13-1P) | Recommended | Required | Required | Required | Required |
| Chevrons (W1-8) and/or One Direction Large Arrow (W1-6) | Optional | Recommended | Required | Required | Required |
| Exit Speed (W13-2) and Ramp Speed (W13-3) on exit ramp | Optional | Optional | Recommended | Required | Required |

**Figure 2. Tables. MUTCD guidelines on Curve Warning Sign Placements**

In summary, the MUTCD Guideline Chapter 2C answers the question as to when, which (the roadway characteristics and traffic conditions), and where (location) a curve's safety-related signs should be placed. To correctly place these signs, the key information variables that need to be collected are the advisory speed, the posted speed, and the curve radius. In the following section, we focus on reviewing the methods to assess and monitor the two variables, advisory speed, and curve radius.

**Curve Advisory Speed Determination**

The curve advisory speed is unarguably the most important factor in terms of horizontal curve safety because the driving speed is the only thing that a driver can control when navigating a vehicle along a curve. It is emphasized that the curve advisory speed is not the safe speed for every type of vehicle under every condition; it is a speed obtained by a defined testing procedure that provides comfort and safety for most driving conditions. In other words, under extreme conditions, such as icy pavements, a driver should evaluate the situation and drive even at a lower speed to avoid danger, e.g., skidding.

It is critical to follow a consistent standard to calculate, design, and set the advisory speed, and through investigation it is found that the "Ball Bank Indicator" (BBI) is the most important factor in establishing the appropriate curve advisory speed. According to the "FHWA method for establishing advisory speed," the "master" equation that computes the safe vehicle speed when negotiating a banked horizontal curve is defined in Equation (1).

This equation can be derived from the law of mechanics and is the foundation of how horizontal curve advisory speeds are set. Equation (1) requires that side friction be a known factor. In practice, the side friction is chosen among three empirical values (0.21, 0.18, 0.15) depending on the driving speed, pavement surface condition, and vehicle type, so the key variables that need to be assessed are the superelevation and the radius. In the following sections of the FHWA publication, six methods to establish the advisory speed are discussed. These methods are as follows:

- Direct Method
- Texas A&M Transportation Institute (TTI) Curve Speed Model – Compass Method
- TTI Curve Speed Model – GPS Method

- TTI Curve Speed Model – Design Method
- Ball-Bank Indicator Method
- Accelerometer Method

The direct method asks a tester to drive over a curve at various speeds and determine the appropriate curve advisory speed subjectively. Historically, the 85$^{th}$-percentile speed of free-flowing traffic is used as the advisory speed, which is no longer explicitly supported by the MUTCD 2009 guidelines. The compass method is used in combination with other methods (e.g., BBI) to determine the curve advisory speed. The purpose of the compass is to obtain the curve radius; therefore, we do not consider it as an individual method to obtain the curve advisory speed. Similarly, the GPS method is used merely to obtain the curve radius and should not be listed individually. The ball-bank indicator method and the accelerometer method are the two methods that are widely adopted and commercialized. They both utilize digital sensors mounted on a vehicle to indirectly calculate the curve safety-related characteristics. In addition to the six methods listed above, there is also a less commonly used Driver Comfort Speed Method, which is the oldest empirical method used to determine a curve advisory subjectively (not considered in this report).

Due to the inefficient and impractical nature of the manual measurement of individual safety properties at horizontal curves, many transportation agencies use ball bank indicator (BBI) values as a composite safety indicator, representing the combined effects from super-elevation, unbalanced lateral acceleration (i.e., side friction), and vehicle body roll. For example, a vehicle equipped with an IMU is driven along a curve at a known speed; then, the curve radius can be indirectly calculated using vehicle kinematic equations.

A network-level BBI measurement is also relatively easier to accomplish than the other methods

presented above. More recently, several studies have tried to estimate BBI using kinematic data acquired from vehicle-mounted cell phones. Notably, a mobile application, “CurveWare,” is available on both Android Play and at the Apple Store as of December 2019; the application seems to be only partially functioning, since the log feature is not working as expected. Also, there is no information on whether the BBI results of this app are validated. We provide the details on estimating the curve radius in the following subsection.

**Curve Radius Estimation**

A survey conducted by Carlson, et. al. (2005) summarized ten common methods to measure curve radius . They can be further classified into four categories: database lookup; field survey; indirect methods; and aerial photographic.

***Database Lookup***

Curve radius is the fundamental characteristic associated with horizontal curves. Since the curve radius remains constant over its lifetime, the most efficient way to acquire curve radius data is to look it up in an agency’s database. Unfortunately, few DOT agencies have created consolidated databases for horizontal curves. Such information is especially scarce for the county-level highway and roads.

***Field Survey***

To measure the curve radius in the field, the starting point (PC) and the ending point (PT) of the curve must be determined first. Next, field operators place a survey rod at safe test points along the inner and outer edges of the curve. At least three test points should be chosen for reliable results. The average of the inner and outer radii will be used as the curve radius. The radius calculated using this method is considered as the ground truth radius and is used to validate other methods.

Measurement of the curve radius in the field can be time-consuming and puts investigators in a dangerous roadway scenario; therefore, there is an urgent need to establish an alternative ground truth method to systematically reduce the number of field survey operations and improve safety.

***Indirect Methods***

Two indirect methods are reviewed. The first is to back calculate the curve radius from the BBI, the vehicle speed, and the superelevation. This requires devices to measure all three variables and might not be as accurate as the other methods because of the measurement error associated with each variable. Note that Equation (2) is simply the rearranged form of Equation (1).

$$R = \frac{\mathrm{V}^2}{15(f + 0.01e)} \tag{2}$$

The other indirect method, the compass method, is known for its simple procedures. Vehicle operators drive along a horizontal curve twice with a compass, once along the inner edge and once along the outer edge; they record the distance traveled with a DMI. Then, the curve radius can be calculated using Equation (3) where *R* is the radius (ft), *L* is the length of the curve (ft), and *Dc* is the difference in the compass headings (degrees):

$$R = \frac{57.3 * L}{D_C} \tag{3}$$

The drawback of the compass method is that it requires an accurate reading of the heading angles, which can only be acquired using expensive electric compasses. Moreover, this method can be only applied to simple curves.

***Aerial Photographic Method***

The easiest way to obtain a single curve radius is to use tools such as Google Maps to directly

measure the curve radius on a map. The main problem with this approach is that it is slow. Another potential issue is the misaligned streets: an aerial map, as shown in Figure 3 aims to preserve the road geometry, but may still subject to projection distortion and imagery offset.

**Figure 3. Picture. Example of aerial imagery offset.**

**Sign Condition Assessment Requirement**

In addition to the correct design and placement of traffic signs, the proper maintenance of these signs is also very important. Minimum safety requirements for traffic signs are provided in the MUTCD (2009). Signs must be properly positioned, clean, undamaged, unobstructed, and legible in daytime and nighttime. According to FHWA (2010), condition assessment should check for missing signs, vegetation blocking signs, cracking, delamination, fading, discoloration, contrast, retro-reflectivity, graffiti, holes, and damaged signposts. Figure 4 shows example images of signs with poor sign physical conditions, such as post-failure, obstructed, faded, dirt, holes, graffiti, and surface failure. Figure 5 shows how poor retro-reflectivity of a sign, which causes poor nighttime visibility. The MUTCD contains the detailed requirements for the minimum retro-reflectivity required for sufficient nighttime visibility for signs and pavement markings.


(Post Failure) (Obstructed) (Faded) (Dirt)

(Holes) (Graffiti) (Surface Failure)

**Figure 4. Pictures. Common distresses in sign condition assessment.**


**Figure 5. Pictures. A sign with low retro-reflectivity which is visible during the daytime but not at night.**

To meet these requirements, an efficient network-level assessment is needed for an updated inventory and timely maintenance and replacement. Sign condition assessment includes both the physical condition of the sign and the sign's nighttime visibility. These factors impact drivers' ability to detect and read signs early enough to make good driving decisions that directly affect

their safety. As outlined in its Transportation Asset Management Plan (2011), GDOT maintains its signs through the Sign Inventory Maintenance System and monitors sign retro-reflectivity to ensure its signs stay above the MUTCD minimums. GDOT performs preventative maintenance such as sign cleaning and vegetation control in addition to daytime and nighttime inspections and replacements when necessary.

In the current practice, there are two commonly used methods of sign nighttime visibility assessment: nighttime visual inspection and nighttime inspection with a handheld retro-reflectometer. FHWA outlines these inspection methods in Methods for Maintaining Traffic Sign Retroreflectivity (FHWA, 2007). The nighttime visual inspection, standard practice for over 50 years, uses a trained two-person crew. The inspector assesses each sign using a vehicle's low-beam headlamps at driving speed and assigns a rating to the sign's brightness and legibility (good, fair, or poor). It is recommended that the inspector to be of older age to more conservatively represent the nighttime vision of drivers. The handheld retro-reflectometer method uses a portable device that can quantify the reflectivity of a sign. According to the ASTM Standard Test Method E1709-00e1, a minimum of four measurements should be taken of the sign background and legend (symbol or lettering). These measurements should then be averaged and compared to the minimum value provided in the MUTCD. Other than these two methods of assessment, FHWA also describes alternative sign management methods that do not require condition assessment: expected sign life and blanket replacement. The expected sign life strategy involves replacing a sign after a specified amount of time based on the sign sheeting warranty or historical data. The blanket replacement strategy replaces all signs in an area or corridor at once. Although some signs may be replaced too early or too late by this method, it is by far the simplest and most affordable strategy because inspection is not needed and effort can be saved

by working in one area at a time. However, for the most effective and reliable asset management, regular empirical condition assessment of signs is needed.

Unfortunately, the existing methods of sign condition assessment have disadvantages. The handheld retro-reflectometer can give objective, quantified measurements of a sign's reflectivity, but using it is time-consuming and requires an inspector to enter a roadway on foot. Additionally, due to its high cost, many agencies cannot afford this technology. Thus, the most common method for sign condition assessment is visual inspection. This method has the advantage of being comprehensive due to its use of human judgment, but it is also very time-consuming, and the results are less repeatable because they are subjective. For efficient and timely network-level condition assessment, there is a need for an automated sign condition assessment method. Georgia Tech (Ai & Tsai, 2014) developed an automated sign condition assessment method using 3D LiDAR technology which can measure the intensity of traffic signs at highway speeds, thus, facilitating the evaluation of sign reflectivity. Using onboard video, there is also potential to use image processing to assess other aspects of the sign condition such as damage, graffiti, obstruction, or post damage.

## CURRENT CURVE SAFETY ASSESSMENT PRACTICES AND CHALLENGES

The following summarizes the discussion with GDOT engineers on field assessment of curve safety conditions. District maintenance crews routinely drive over the roadways and make engineering judgments based on their knowledge of roadway guidelines (AASHTO, MUTCD, GDOT Signing, and Marking Guide, etc.) to proactively assess safety concerns on curves (such as insufficient sight distance, lack of signs, poor pavement condition, missing striping, insufficient super elevation, etc.). GDOT also responds to citizen concerns (for example, people

report frequent crashes on specific curves), investigates the locations, and identifies unsafe curves. After the maintenance crews identify the safety concerns on the curves, they notify the GDOT Office of Traffic Operation. The Office of Traffic Operations investigates the reason/issue, evaluates the situation, and determines the suitability of signage to resolve the safety concerns. If new signs are required, the Office of Traffic Operations then approves new signage and the new signs are installed by the maintenance crews.

District maintenance crews routinely drive over the roadways and assess the existing signs. Because they are familiar with the roadways and their requirements for good, safe signage, most of the time, GDOT personnel recognize missing signs. They also assess the existing signs for damage and fading. In addition to physical sign conditions, they assess the retro-reflectivity condition of the signs by an annual nighttime visual inspection. Roadway maintenance crews are tasked with the upkeep of signage in their areas (including reflectivity); they are responsible for any signs that are damaged/removed. If a sign is knocked down/missing, damaged, or old/faded, the maintenance office will replace the sign.

The following summarizes the challenges in the current practices.

1. It is difficult to visually assess curve radius in the field. With the use of the Curve Advisory Reporting System (CARS), it is still time-consuming to extract detailed curve information, including radius, point of curve (PT) and point of Tangent (PT), because of its subjective, trial-and- error curve fitting nature. There is a need to develop a method that automatically extracts detailed curve information. The CARS software is currently commonly used by commonly by transportation agencies to extract curve information.
2. Current in-service curve safety assessment practice are, largely, manual operations based on visual inspection, which are ineffective. However, the change of roadway characteristics,

like superelevation, caused by pavement resurfacings, is difficult to be identified visually. There is a need to have an automatic way to measure curve roadway characteristics, like superelevation.

3. Ball Bank Indicator (BBI) angles are important roadway safety indicators and are commonly used to assess curve safety conditions and to make recommendations for applying curve safety countermeasures, like the applications of High Friction Surface Treatment (HFST). However, collecting BBI data with dedicated vehicles and designated engineers is time-consuming and labor-intensive. There is a need to develop an enhanced method, such as one that uses smartphones to collect BBI values.
4. Current practices in determining advisory speeds on curves are time-consuming and labor-intensive. The roadway BBI angle, superelevation, and curve radius need to be acquired to determine a curve's adequate advisory speed. There is a need to develop an enhanced method to perform advisory speed computation.
5. Currently, missing signs are identified by district maintenance crews as they perform their routine inspection duty. However, it is very time-consuming and challenging for crews to thoroughly assess each curve sign based on required sign types and spacing on each curve along a route and identify missing signs. Therefore, there is a need to develop an automatic curve sign detection and classification and digitally compare them with curve sign requirement specified in the MUTCD to cost-effectively identify missing signs.

# CHAPTER 3. ENHANCED NETWORK LEVEL CURVE SAFETY ASSESSMENT METHOD USING LOW-COST MOBILE DEVICES

This chapter presents our proposed method to conduct curve safety assessments for advisory speed limit determination at the network level using low-cost mobile devices. The flow chart of the overall data collection and computational framework is presented in Figure 6.

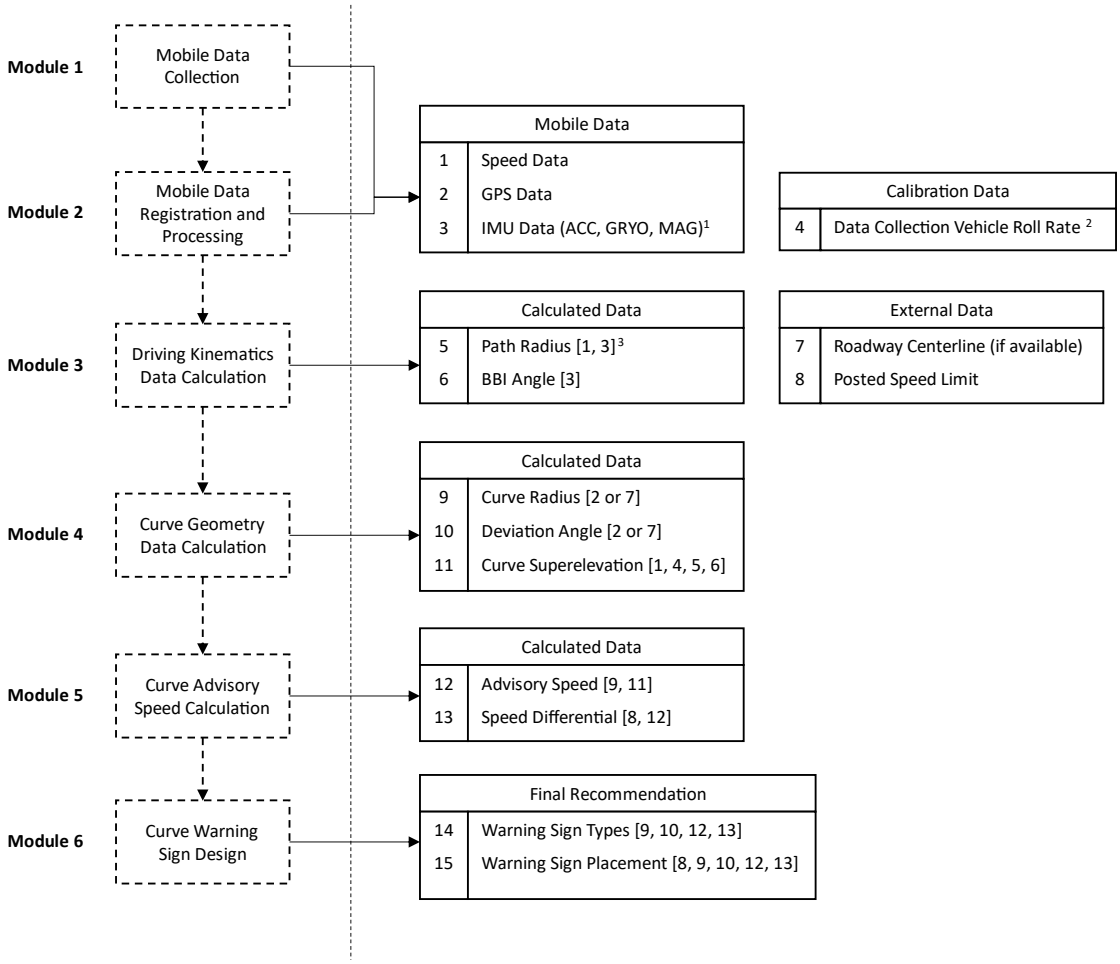


[1] : IMU data includes accelerometer, gyroscope, magnetometer readings
[2] : Vehicle roll rate refers to the stiffness constant for computing vehicle body roll angle under lateral load
[3] : Numbers listed in the brackets refer to the data item(s) needed for obtaining the current data item

**Figure 6. Flowchart. Data collection and computational framework and data items for network-level curve safety assessment using mobile devices.**

There are six modules presented in this framework: mobile data collection, mobile data registration and processing, driving kinematics calculation, curve geometry calculation, advisory

speed calculation, and curve warning sign design. In Module 1, mobile devices are used to collect vehicle speed, global positioning system (GPS), and inertial measurement unit (IMU) data. The collected data are registered and processed in Module 2. In Module 3, data items related to the driver inputs and the interactions between vehicle and roadway (driving kinematics data) are computed; this data includes the path radius of the driving trajectory and the BBI angle during the data collection. After driving kinematics data is processed, curve geometry data is computed in Module 4. While the data collected by the mobile device itself (without knowing vehicle's roll rate) is enough to estimate roadway superelevation, better results can be obtained if the vehicle's roll rate, a property related to the vehicle's suspension, is available to calibrate the superelevation results. In addition, in order to obtain the curve radius and the curve deviation angle, it is recommended that the curve centerline be used as external data input for computing these data items. With curve geometry data obtained, the advisory speed and the speed differential can be computed (with posted speed limit as external data input) as shown in Module 5. Finally, in Module 6, the computed data outcome from previous modules can be used to provide a curve warning sign design that provides proper warning sign selection and placement. This chapter focuses on using the data collected by the mobile devices to compute the data items in Modules 1-5 to support MUTCD curve warning sign design. The chapter also propose a new calibration method to estimate vehicle roll rate to compensate superelevation computation by considering the impact of vehicle body roll.

## MODULE 1: MOBILE DATA COLLECTION

A mobile application "AllGather" was developed by Georgia Tech for mobile data collection and storage of the GPS trajectory, vehicle speed, IMU data, and onboard camera view during the data collection.

The vehicle speed, GPS trajectory, and IMU data are stored in CSV format and used in the computational framework. The IMU data collected from the mobile devices includes three-axis (XYZ) readings of accelerometer, gyroscope, and magnetometer. This data can be used to describe the vehicle's motion when driving; therefore, it is used to compute driving kinematics data, such as the driving path radius and the BBI angle. The three-axis readings of the IMU data use the mobile device's local reference frame as the coordinate system, as shown in Figure 7. The vehicle speed, GPS, and IMU data are pulled and recorded using Android's recommended library functions. The accelerometer and magnetometer measure the linear acceleration and magnetic field strength along each of the three axes, and the gyroscope measures the angular velocity around each axis. Since the axes use the mobile device's local reference frames, they do not change with the smartphone's orientation; therefore, to use the IMU data from the mobile device to describe the vehicle's motion, the mobile device must be fixed to the vehicle to keep the local reference frames of the mobile device and the vehicle aligned.

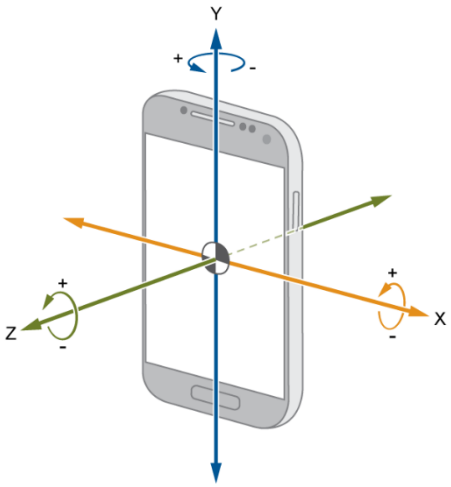


**Figure 7. Diagram. Typical coordinate system for mobile device's IMU.**

The camera of the mobile device is used to record video during data collection of such data roadway image data that is useful for visualizing curve site conditions and data collection

conditions; furthermore, the video log collected can also be used to detect and inventory traffic signs and other roadside assets, such as guard rails and retaining walls. Figure 8 shows an example setup of the mobile device using a windshield mount. The camera data collected using the AllGather application is stored in MPEG4 video format.

**Figure 8. Picture. Example setup of AllGather application.**

## MODULE 2: MOBILE DATA REGISTRATION

Data registration is the procedure that aligns two or more data tables generated from different sensors or devices so that they share the same index column. For temporal data registration, the index column is the timestamp, and for spatial data registration, the index column can be GPS points or the linear referencing distance on a roadway centerline. This section presents the methods to temporally register data collected by different sensors in a single data collection run and spatially register the collected data in multiple data collection runs.

### Temporal Data Registration

In single runs of data collection, the mobile data collection records readings from different sensors (GPS and IMU); even though the sensors share the same system clock, temporal data

registration is still needed due to different sensors possibly having different sampling rates. For example, typical Android devices can report GPS data at a 1-Hz sampling frequency, while IMU data can be refreshed at higher frequency (e.g., 10 Hz). This will result in data tables that have different lengths for the same time period. Therefore, in order to have correlated IMU data at each GPS point, and vice versa, both data tables are resampled at a common timestamp with the same sampling frequency.

Figure 9 illustrates how two data tables are registered so that they share the same timestamps. The two data tables are first combined using the *outer join* operation, creating a super table that has one single timestamp column that contains the timestamps from both Raw Data from Device A and Raw Data from Device B. In the resulting Merged Data Table, the missing data (corresponding to the timestamp that only show up in one of the input tables) are created using linear interpolation. Finally, the Merged Data Table is resampled at a fixed frequency (e.g., 2 Hz) using averaged values to produce the registered data table.

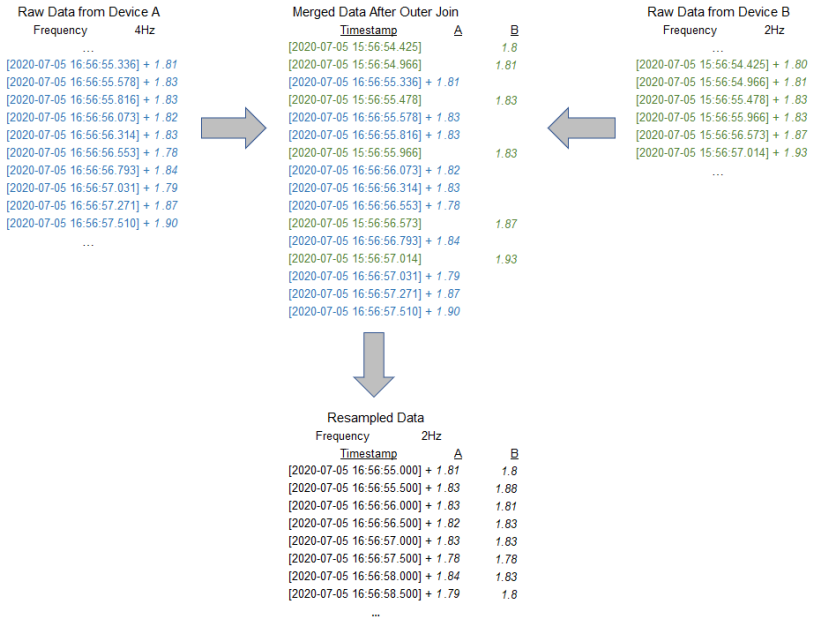


**Figure 9: Illustration. Temporal data registration of data tables with different sampling frequencies.**

### Spatial Data Registration

In multi-run data collection, although the data collected in each individual run can be registered using temporal registration, the data from run to run do not share common timestamps. Therefore, to enable multi-run data aggregation, comparison, and analysis, spatial data registration is needed. The goal of spatial registration is to merge data tables so that the resulting table has a common GPS or spatial index column.

The process of spatial data registration is very similar to the temporal registration; the difference is that the spatial information is used as the common index. There are two types of spatial information that can be used as a spatial index: GPS and linear referenced distance. The benefit of using GPS as the spatial index is that GPS data are readily available from the collected data with no pre-processing needed; in order to get linear referencing distance, the GPS points need to be projected onto a roadway centerline before the linear referencing distance can be computed. However, since curve inventory data can define a curve segment using the linear referencing distance of the PC and PT points, using the linear referencing distance can be useful for querying data related to a specific curve. Other than the difference in what is being used as the common index, the spatial data registration procedure is essentially the same as the temporal data registration.

## MODULE 3: DRIVING KINEMATICS DATA CALCULATION

The kinematics data items included in the computational framework include the path radius and BBI angle. It is worth noting that, in the proposed computational framework (Figure 6), there are two types of radius data: path radius and curve radius. Radius estimation is a crucial step of the computational framework, and it is important to understand the difference between the two types

of radius data, as the path radius and curve radius should not be used interchangeably for computing curve superelevation and determining an appropriate curve advisory. During cornering, as the vehicle wanders laterally within the lane, the curvature of the vehicle path can be different from the geometry radius of the curve. As illustrated in Figure 10, an experienced driver may use lateral movement within the lane to "flatten" the curve so the path's curvature, the inverse of radius, is smaller than the curve centerline's curvature. Similarly, an inexperienced driver or a driver who makes a poorly executed turns by "jerking" the steering wheel may cause the path curvature to be temporarily larger than the curve centerline's curvature. Therefore, in the computational framework, we propose to use the path radius to reflect the driving trajectory and the curve radius to reflect the curved roadway geometry.

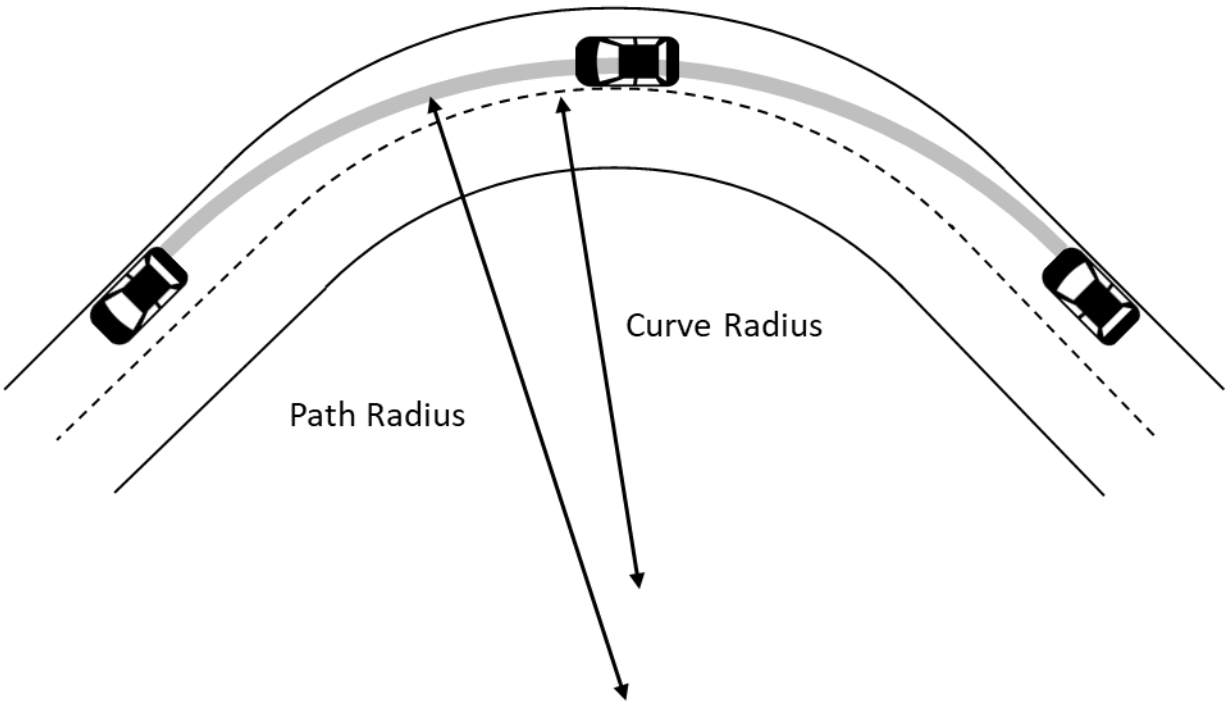


**Figure 10. Illustration. Difference between path radius and curve radius due to lateral movement within the lane.**

**Path Radius Estimation Using Vehicle Speed and Angular Velocity**

As illustrated in Figure 10, path radius is largely dependent on the steering input from the driver, and the path radius can easily change from one moment to another based on the driver's input. Therefore, the measurement of the path radius should reflect the vehicle's movement at a particular instant. Given the fact that at least three GPS points are mathematically required for estimating the trajectory radius, meaning the result is not based on an instance but a period, and GPS accuracy may cause numerical instability in radius results when too few points are used, making GPS points sub-optimal data for the path radius estimation. Fundamentally, the movement of a vehicle's cornering is the combined result of the vehicle's moving forward and rotating around its vertical axis at the same time. Since the IMU data collected by the mobile devices include readings from the gyroscopes, which report the angular velocity around each of the three-dimensional axes, the path radius can be estimated by using the vehicle's travel speed and gyroscope readings. As shown in Figure 11, assuming the vehicle is not spinning (oversteering) on the curve, the path radius at any given point can be expressed as the ratio between the travel speed and angular velocity of the vehicle's vertical axis. As the travel speed and angular velocity are tied closely to the vehicle's motion at a particular moment, this method of estimating a vehicle's path radius is a better approach for obtaining instantaneous path radius.

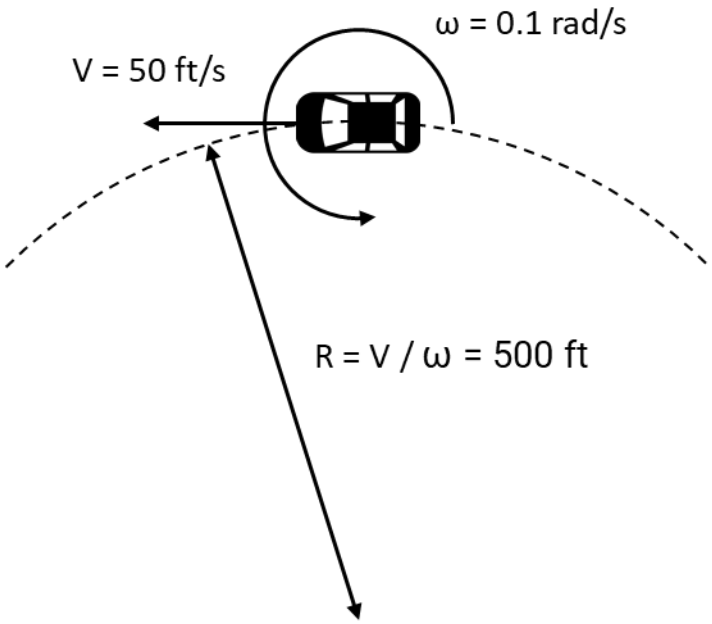


**Figure 11. Illustration. Relationship between path radius, vehicle speed, and angular velocity.**

**Curve Driving Kinematics**

This section briefly describes the kinematics of curve driving to lay the foundation for BBI computation and superelevation computation using the BBI angle. To illustrate the kinematics of curve driving, this section largely references the Appendix A of the "Development of Guidelines for Establishing Effective Curve Advisory Speed" (Bonneson et al., 2007).

The Ball-Bank Indicator angle (BBI angle) refers to "the movement of the ball is measured in degrees of deflection, and this reading is indicative of the combined effect of superelevation, lateral (centripetal) acceleration, and vehicle body roll" (Milstead et al., 2011). Figure 12 illustrates the relationship between the BBI angle (**α**), the lateral acceleration ($\boldsymbol{m}\frac{\boldsymbol{V^2}}{\boldsymbol{R}}$), superelevation angle (**ϕ**) and a vehicle's body roll (**ρ**).

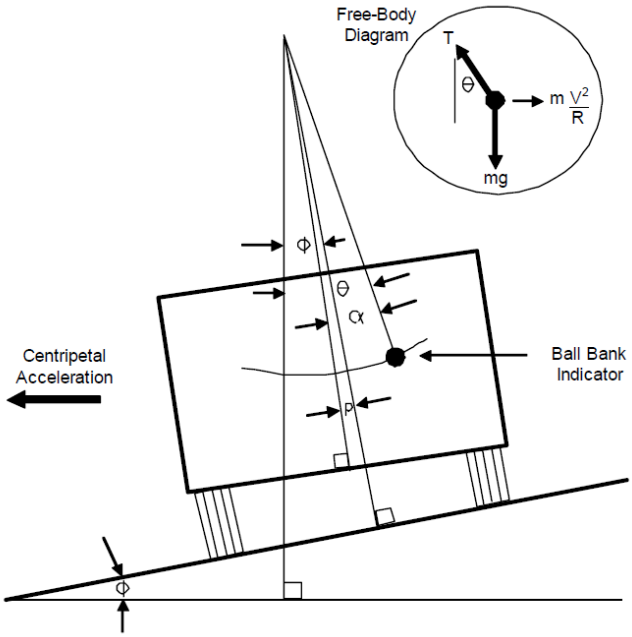


**Figure 12. Diagram. Interaction between BBI and superelevation, lateral acceleration, and vehicle body roll. (Bonneson et al., 2007)**

The relationship shown in Figure 12 is valid at any timestamp when a vehicle is on a curve, and this can be expressed as Equation (4).

$$\frac{\left(1.47 * V(t_i)\right)^2}{gR_p(t_i)} = \tan\left(\alpha(t_i) + \Phi(t_i) - \rho(t_i)\right) \quad (4)$$

Where,

$\alpha(t_i)$ = ball-bank indicator angle at $t = t_i$, radians;
$\Phi(t_i)$ = superelevation angle at $t = t_i$, equitant to atan $(\frac{e}{100})$, radians;
$\rho(t_i)$ = body roll angle at $t = t_i$, radians;
$V(t_i)$ = vehicle travel speed at $t = t_i$, mph;
$R_p(t_i)$ = vehicle path radius at $t = t_i$, ft;

From Figure 12, we can see that the angle **θ** is caused by the centripetal acceleration, while the superelevation supplies a portion of the acceleration; the remaining portion is supplied by the tire-pavement side-friction. As the angle **ϕ** represents the superelevation angle, we can define a side-friction angle ($\boldsymbol{f_r}$) as the difference between the lateral acceleration angle and the

superelevation angle ($\boldsymbol{\theta - \phi}$). Therefore, the relationship in Equation (5) can also be derived.

$$f_r = \text{atan}\left(\frac{\left(1.47 * V(t_i)\right)^2}{gR_p(t_i)}\right) - \text{atan}\left(\frac{e(t_i)}{100}\right) \quad (5)$$

We can also see in Figure 12 that the BBI angle ($\boldsymbol{\alpha}$) is closely related to the side-friction angle ($\boldsymbol{f_r}$) with the inclusion of the vehicle body roll angle ($\boldsymbol{\rho}$).

$$\alpha(t_i) = f_r(t_i) + \rho(t_i) \quad (6)$$

The vehicle body roll is caused by the lateral load acting on the vehicle; the amount of body roll under the same lateral load is heavily dependent on the vehicle's suspension properties. Research by Moyer and Berry (1940) revealed a constant roll rate can be found between side-friction angle and body roll angle. This relationship is shown in Equation (7), where k = roll-rate of the vehicle (rad/rad).

$$\rho(t_i) = k * f_r(t_i) \quad (7)$$

Subsequently, the relationship between the BBI angle and the side-friction angle can be expressed as Equation (8)

$$\alpha = f_r(t_i) * (1 + k) \quad (8)$$

And substitute side-friction angle in Equation (8) with Equation (5), Equation (9) can be derived.

$$\alpha(t_i) = \left(\text{atan}\left(\frac{\left(1.47 * V(t_i)\right)^2}{gR_p(t_i)}\right) - \text{atan}\left(\frac{e(t_i)}{100}\right)\right) * (1 + k) \quad (9)$$

It is worth noting that when a vehicle's roll rate is not available, assuming the vehicle roll rate

equals to zero is equivalent to assuming no body roll when the vehicle is turning and using this assumption to estimate the side-friction angle from the BBI angle will exaggerate the side-friction angle. The amount of error from this assumption will increase as the BBI angle increases because the amount of error and the BBI angle have a positive linear relationship.

It is also worth noting that what Equation (9) represents is that when a vehicle's speed, path radius, and superelevation are known, the side-friction angle can be computed; it should have a (1+k) relationship to the BBI angle, and when the vehicle roll rate is also known, the expected BBI angle can be computed to validate the BBI angle as computed from the mobile device's BBI angle.

**BBI Angle Computation**

After understanding the curve driving kinematics, we can see the BBI angle is the angle between the vehicle chassis' vertical direction and the net acceleration (including gravity) experienced by the vehicle. Therefore, the two items needed for computing the BBI angle from mobile data are vehicle chassis' vertical direction vector ($\vec{\boldsymbol{G}}$) and the net acceleration vector ($\vec{\boldsymbol{A}}(\boldsymbol{t_i})$). The chassis' vertical direction vector represents the direction of the net acceleration vector and if they are parallel, it would result in a "zero" BBI reading; thus, this vector will be referred to as the "zero vector" in the rest of this report.

To obtain the "zero vector", the data collection device must be first fixed to the vehicle's chassis (e.g., mounted to the windshield using a suction cup holder), with the camera facing forward. The vehicle must remain stationary on level ground for the first few seconds of a data collection run. During the stationary phase, the direction of the gravity is being measured by the accelerometers and used as the "zero vector".

After the "zero vector" is obtained, the accelerometers continuously measure the acceleration experienced by the vehicle, and the acceleration component perpendicular to the vehicle's driving direction is used for computing the BBI angle. The BBI angle computation is expressed as shown in Equation (10).

$$\alpha(t_i) = arctan2\big(Det(\vec{G}, \vec{A}(t_i)), Dot(\vec{G}, \vec{A}(t_i))\big) \quad (10)$$

## MODULE 4: CURVE GEOMETRY DATA COMPUTATION

This section presents the computational procedure for calculating curve geometry data. The curve radius and deviation angle are computed from the roadway's centerline or GPS data; the curve superelevation is computed from IMU data.

### Curve Radius and Deviation Angle Estimation

The curve radius and curve deviation angle of the roadway can be estimated by fitting a circle on the geometric shape of the road centerline or GPS trajectory. Typically, three major steps are involved:

Step 1: Centerline or trajectory data smoothing,

Step 2: PC and PT identification, and deviation angle estimation.

Step 3: Radius estimation.

Step 1 is to remove the outliers from the raw centerline and GPS data because the PC and PT identification is highly relying on the change of heading, which is computed by consecutive points rolling along the data. The polynomial approximation with exponential kernel (PAEK) method is a smoothing algorithm developed by ESRI ArcGIS software that provides a stable line-smoothing function. This function is developed based on the algorithm defined by

Bodansky, et al, (2002).

Step 2 is to identify the PC and PT based on the change of heading. A vehicle's heading starts changing at PC and stops at PT. The change of heading can be computed as the difference of the bearing angle between consecutive points. Figure 13 shows the centerline data with extracted curves on State Route 2 (SR-2), and Figure 14 shows the bearing angle with extracted curves correspondingly.

Step 3 is to fit the circle between PC and PT to estimate the radius for each extracted curve. The Kasa method is a widely used least-squares circle geometric fitting method that is based on finding the minimum distances from the given points to the geometric feature to be fitted (Kåsa, I., 1976).

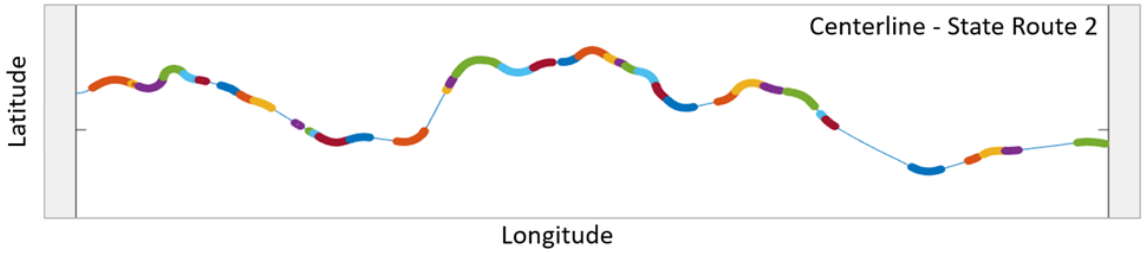


**Figure 13. Plot. Roadway centerline with extracted curves on part of State Route 2.**

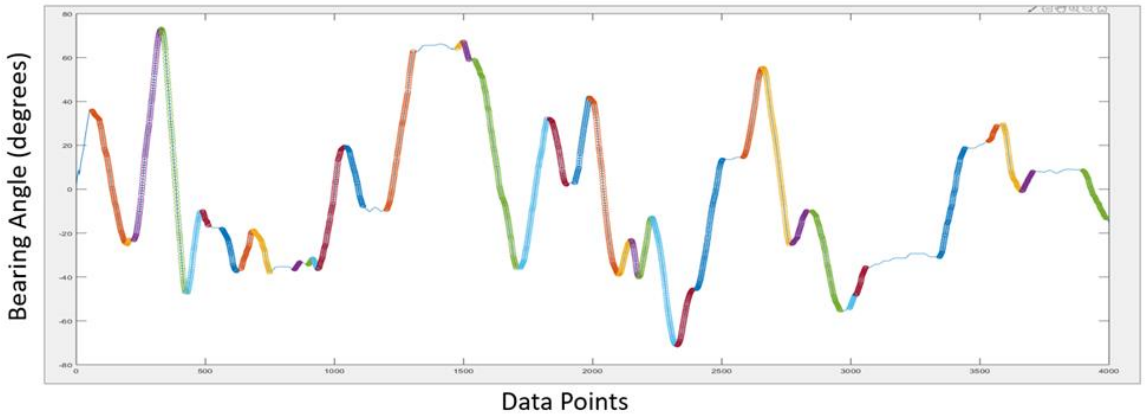


**Figure 14. Plot. Bearing angle with extracted curves on part of State Route 2.**

### Curve Superelevation Computation

From Equation (9), the computation for superelevation can be derived as Equation (11). Note that the relationship in Equation (11) is based on any arbitrary instance of the vehicle's motion state; therefore, the path radius at a timestamp ($\boldsymbol{R_p(t_i)}$) is used to represent the vehicle's motions state.

$$e(t_i) = 100 * \tan\left(\operatorname{atan}\left(\frac{\left(1.47 * V(t_i)\right)^2}{gR_p(t_i)}\right) - \frac{\alpha(t_i)}{(1+k)}\right) \quad (11)$$

Note that a positive BBI angle should have a positive sign when the BBI reading indicates the "steel ball" is swinging towards the outside of the curve, and a negative sign should be used when the "steel ball" swings toward the inside of the curve.

## CALIBRATION METHOD FOR VEHICLE ROLL RATE ESTIMATION

As shown in Equation (11), the vehicle speed, path radius, BBI angle, and vehicle roll rate are needed for superelevation computation. The vehicle speed, path radius, and BBI angle can either be directly obtained or computed from the collected mobile data. The vehicle roll rate ($\boldsymbol{k}$) cannot be directly measured by the mobile device. As discussed in the Curve Driving Kinematics section, assuming $\boldsymbol{k} = 0$, reasonable superelevation results may still be obtained, but the error of superelevation will continuously grow with higher and higher side-friction angles. In other words, for the same curve, as the driving speed increases, the superelevation results will be more and more underestimated.

Two calibration procedures for vehicle roll rate estimation through the mobile data collection are presented in this section. The first method requires the superelevation to be measured; the second method does not require known superelevation, but it would require multi-run data collection on

the same curve at different driving speeds.

**Calibration Using Curves with Known Superelevation**

As shown in Equations (5) and (8), the side-friction angle ($\boldsymbol{f_r}$) can be determined with the known vehicle speed, path radius, and superelevation. The resulting side-friction angle ($\boldsymbol{f_r}$) would also have a $(1 + \boldsymbol{k})$ relationship with the measured BBI angle. Therefore, when the superelevation is known, the side-friction angle can be calculated using the known superelevation for locations where BBI angle data was measured, the side-friction angle and BBI angle would show a linear relationship with the slope equal to $(1 + \boldsymbol{k})$.

Figure 15 shows an example outcome from tests performed by the research team on the National Center of Asphalt Technology (NCAT) test track. The superelevation was manually measured at 100-ft-stations on spiral sections and 200-ft stations on constant radius sections. The measured superelevation was combined with collected mobile data to compute the side friction angle and showed a good linear relationship with the computed BBI with a slope equal to 1.093, indicating the data collection vehicle had a roll rate of 0.093 rad/rad. Detailed results of using this calibration method are presented in Chapter 4.

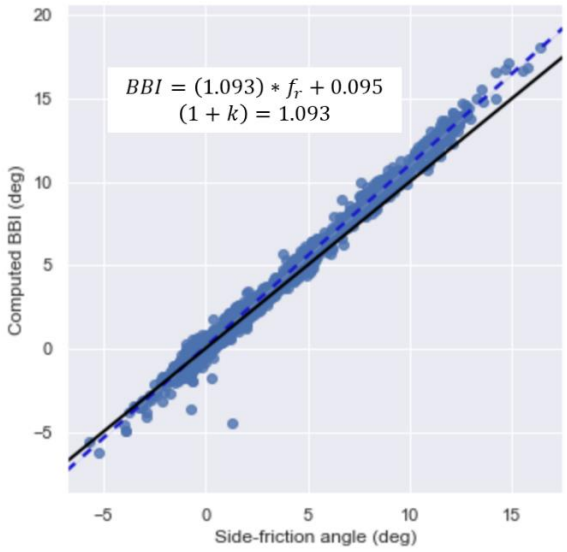


**Figure 15. Chart. Example relationship between computed BBI and side-friction angle on NCAT test track with manually measured superelevation.**

### Calibration Using Curves with Unknown Superelevation

Considering that manually measuring curve superelevation might be impractical for agencies without access to a closed facility, another calibration method can be used. Multiple runs of data can be collected at different speeds on the same curve with unknown superelevation. This method works because the superelevation does not change for the same curve between multiple passes**.** Although the true superelevation is unknown, if vehicle roll rate is estimated correctly, the computed superelevation should be similar between runs at different speeds.

In practice, this calibration method first uses spatial registration to find data points from different data collection runs that correspond to the same locations on a curve. Then, constructing a set of equations using Equation (11) with both the roll-rate and superelevation as unknowns.

Equation (11) can be written as Equation (12) to illustrate that when superelevation $\boldsymbol{e(t_i)}$ is a constant, the term $\mathbf{atan}\left(\frac{(1.47*V(t_i))^2}{gR_p(t_i)}\right)$ and the BBI angle $\boldsymbol{\alpha(t_i)}$ have a linear relationship with a slope equal to $\frac{1}{(1+k)}$.

$$\operatorname{atan}\left(\frac{\left(1.47 * V(t_i)\right)^2}{g R_p(t_i)}\right) = \operatorname{atan}\left(\frac{e(t_i)}{100}\right) + \frac{1}{(1+k)} * \alpha(t_i) \qquad (12)$$

Therefore, using a linear regression algorithm, the best fit solution of the roll rate for the given multi-run data can be found.

The data presented in Figure 15 were collected at five different speeds in 5 mph increments. Using the same data, but without using the measured superelevation, this calibration method finds a best-fit vehicle roll-rate equal to 0.095 rad/rad, similar to the roll-rate found in using the "Known Superelevation" method of 0.093. Detailed analysis of this calibration method is presented in Chapter 4.

## MODULE 5: ADVISORY SPEED DETERMINATION

### Advisory Speed Determination from Single-Run Data Collection

Accurate computation of the curve advisory speed is critical to driver safety because it determines the type and placement of warning signs. If the computed advisory speed is too high, drivers may be unprepared for the sharpness of a curve. If the computed advisory speed is too low, drivers will lose their trust in the curve warning signs and begin disregarding them, ultimately putting themselves in danger. Equation (13) shows the calculation for determining the curve advisory speed. Note that curve radius ($\boldsymbol{R_c}$), not path radius ($\boldsymbol{R_p}$), is used in this calculation, as the advisory speed is dependent on the curve geometry, not a particular driver during a particular data collection run.

$$V_{adv} = \sqrt{15 * \left(\frac{e}{100} + f_{max}\right) * R_c} \quad (13)$$

Where,

$f_{max}$ = maximum allowed side friction factor by the advisory speed criteria;

$R_c$ = curve radius, ft;

$V_{adv}$ = advisory speed limit, mph.

The MUTCD 2009 edition defines the advisory speed criteria as follows:

- 16 degrees of ball-bank for speeds of 20 mph or less,
- 14 degrees of ball-bank for speeds of 25 to 30 mph, and
- 12 degrees of ball-bank for speeds of 35 mph and higher.

This corresponds to the maximum allowed side friction factors as follows:

- 0.287 for speeds of 20 mph or less,
- 0.249 for speeds of 25 to 30 mph, and
- 0.212 for speeds of 35 mph and higher.

For single-run collected data, the advisory speed can be calculated for each data point along a curve, and the lowest advisory speed result will be reported as the advisory speed of the curve.

**Advisory Speed Determination from Multiple-Run Data Collection**

For multi-run collected data, each individual data collection run will be processed using the proposed computational framework. Since an advisory speed is determined based on the minimum advisory speed results along the curve, any noise or unreliable data will almost always lower the overall advisory speed for the curve; therefore, for multi-run data processing, the

highest advisory speed from the individual single runs should be used as the advisory speed of the curve. In addition, variations between individual runs can be used as indicators for flagging unreliable results that are recommended for data re-collection. The outcome of the final advisory speed is determined by comparing the advisory speeds derived from the multi-run data. Besides choosing the one with highest advisory speed. A confidence level (L, M, and H) of the computed advisory speed is recommended based on the variability among the computed single-run advisory speeds. This confidence level is a qualitative indicator. For a low confidence level (L), it means that there is a high variability among different runs of data. In some cases, re-collecting the data in the field is recommended because of high data variability. A high confidence level indicates that there is a high consistency on different runs of measurements. Chapter 5 presents a case study on multi-run analysis using data collected on Georgia State Route 17. In the current computational framework, the multiple-run data being used is based on the advisory speed outcome. The rich data collected in the multi-run mobile data collection still has a huge potential to be used for other analyses that can be used to determine data quality or even study driver behavior.

## SUMMARY

This chapter presented the proposed data collection and computational framework for curve safety assessment and advisory speed determination using low-cost mobile devices. The chapter also presented the theoretical foundations of the data calculations to show the feasibility of the framework. Especially, the chapter presented an innovative calibration procedure to estimate vehicle roll rate for improving the accuracy of superelevation computations. In the following chapters, validation of the proposed framework and a case study using the proposed framework will be presented.

# CHAPTER 4. VALIDATION OF PROPOSED COMPUTATIONAL FRAMEWORK USING MOBILE DATA COLLECTION DEVICES

This chapter presents the validation tests and results of the proposed computational framework for curve safety assessment using mobile data collection devices. Two tests are presented in this chapter, a repeatability test to perform a preliminary evaluation of the mobile sensor's repeatability across different devices, and a validation test to comprehensively evaluate the performance using mobile devices in the proposed computational framework. The validation test was performed at National Center for Asphalt Technology (NCAT) closed test track, with the goal of validating the proposed method using different driving speeds and driver inputs. This chapter will evaluate the computed results of the radius, BBI angle, superelevation, and advisory speed. Using the proposed method to evaluate the feasibility of estimating superelevation with low-cost smart phones, the validation test was centered around comparing the computed superelevation results with the manually measured track superelevation. The logic behind this design is two-fold. First, superelevation is an important element in curve geometry information needed to determine appropriate curve advisory speed. Its accuracy is dependent on other computed elements, such as path radius and BBI angle; therefore, an accurate superelevation estimation would require accurate estimation of both the path radius and the BBI angle. Second, superelevation, as part of the curve geometry, can be physically measured and does not change during the test with different travel speeds or different driver inputs. This makes the evaluation of the proposed method straightforward, as data collected from different data collection runs can be compared to the same ground reference superelevation values.

## REPEATABILITY TEST OF THE MOBILE SENSORS

The reliability and repeatability of mobile sensors are fundamental to the use of mobile devices for curve safety assessment data collection. In this test, the goal is to evaluate the repeatability of the IMU data collected by multiple mobile devices in the same data collection environment. The test was designed to place a number of mobile devices in the same orientation within the data collection vehicle and record the IMU data as the vehicle was driven. The test was set up, as shown in Figure 16, by placing three smartphones on the dashboard. Three different smartphones were used: the Xiaomi Redmi Note 4 White (Xiaomi 1), Google Pixel 3a (Pixel), Xiaomi Redmi Note 4 Black (Xiaomi 2).

**Figure 16. Picture. Device setup for multi-device sensor repeatability test.**

Since these smartphones were all placed in the same vehicle during the same data collection, the data collection environment is identical for all the devices. In other words, if the data collected by different devices was perfectly repeatable, the IMU data collected by the different devices should have a perfect correlation among the devices.

The IMU data in each device reports the linear acceleration, angular velocity, and magnetic fields in all XYZ directions. However, the proposed computational framework only requires linear acceleration and angular velocity data from the IMU. For each of the sensor readings, the normalized cross-correlation was compared for each pair of devices. Normalized cross-correlation measures the similarity between two signals and is bounded between -1 and 1; a

correlation of 1 indicates the signals have a perfect similarity. Table 1 shows the normalized cross-correlation of different sensor data between different pairs of devices.

**Table 1. Correlation of collected sensor data between different devices.**

| | Normalized Cross-Correlation | | |
|---|---|---|---|
| **Collected Data** | **Xiaomi1 & Xiaomi2** | **Xiaomi1 & Pixel** | **Xiaomi2 & Pixel** |
| Linear acceleration X | 0.9805 | 0.9638 | 0.9961 |
| Linear acceleration Y | 0.8431 | 0.9225 | 0.9845 |
| Linear acceleration Z | 0.9998 | 0.9997 | 0.9997 |
| Angular velocity X | 0.9921 | 0.9436 | 0.9516 |
| Angular velocity Y | 0.9948 | 0.8000 | 0.8036 |
| Angular velocity Z | 0.9999 | 0.9996 | 0.9997 |

From the results, we can see that the majority of the sensor data has a high (more than 0.98) correlation, indicating results computed from the data collected by one mobile device can be repeated by another mobile device. Among different sensors, the angular velocity in the Y direction showed the lowest normalized cross-correlation value. This is likely due to the way the devices were set up in Figure 16; the Y-axis of the devices was aligned with the driving direction, and in typical driving conditions, the vehicle does not rotate significantly around this axis. Therefore, there was no significant rotation signal for the sensor to collect and the correlation score was largely impacted by the random noise of the sensor. Given that the sensor qualities within the same device are generally similar, the repeatability of the angular velocity Y should be similar to other axes if the device was orientated differently in the vehicle.

## VALIDATION TEST OF THE PROPOSED METHOD

The purpose of the validation test was to evaluate the feasibility of the proposed method which uses mobile devices for curve safety assessment data collection and analysis.

This test focused on validating the superelevation estimation accuracy. Superelevation is an important data item for determining the appropriate curve advisory speed, and superelevation is

part of the curve geometry that can be physically measured to evaluate the superelevation estimation accuracy. Evaluation of other computed data items, such as the BBI angles and advisory speed limit, was expanded from the superelevation by using manually measured superelevation to back-calculate the expected values.

**Validation Test Location National Center for Asphalt Technology (NCAT)**

The National Center for Asphalt Technology (NCAT), located in Auburn, Alabama, has a closed facility with a 1.7-mile oval test track for accelerated pavement tests (shown in Figure 17). NCAT's test track is an ideal site for performing the validation test, as the superelevation can be manually measured without the need for traffic control, since the test track is not on public roads. In addition, horizontal alignment and cross-section drawings are available to provide curve geometry information. However, since the test track has been repaved multiple times after its initial construction, the superelevation values were manually measured throughout the curve to obtain the current superelevation on the test track.

**Figure 17: NCAT Test Track (Google Earth).**

**Validation Test Design and Test Procedure**

As stated previously, while the purpose of the test was to validate the computed data items in the proposed computational framework, the design of the validation was focused on using

superelevation as the physically measurable curve geometry to validate the superelevation computation; the validation also used the measured superelevation to back-calculate the expected values for validating the BBI angle and advisory speed computation. In addition, the validation of the curve radius estimation was done by comparing the estimated curve radius to the radius documented in the track design drawing.

### *Manual Superelevation Measurements*

To obtain detailed superelevation data on the NCAT test track, superelevation was measured throughout the curves. The curves on the NCAT test track are composed of one constant radius portion in the middle of the curve with a radius of 476 feet, and two spiral proportions at the beginning and the end of the curve to transition to the tangent parts of the track. The superelevation data was measured every 200 feet on the constant radius section and every 100 feet on the spiral sections; additional measurements were made at transition points between tangent and spiral sections and between spiral and circle sections. Figure 18 shows the locations on the NCAT test track where superelevation was manually measured.

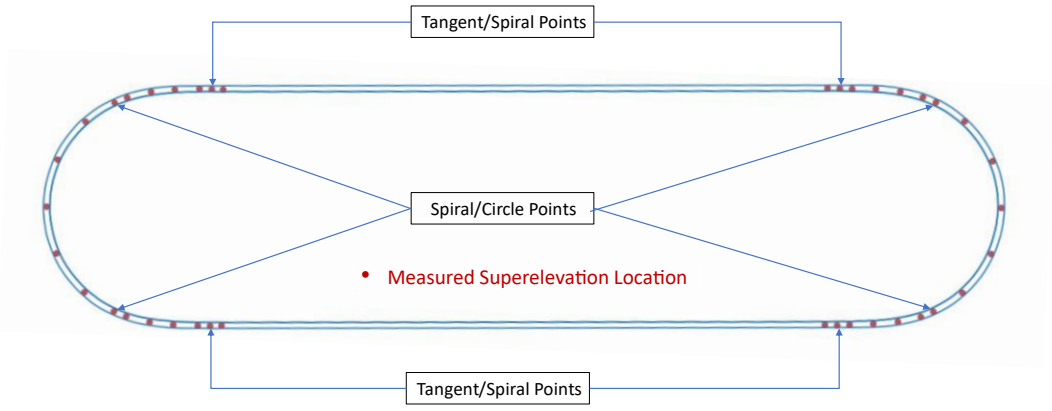


**Figure 18. Diagram. Locations on the NCAT test track where superelevation is manually measured.**

At each location shown in Figure 18, superelevation measurements were manually taken using

an 8-ft straightedge and a digital level; three measurements were taken at each location with 1 ft between each location. Averages of the three measurements were used to represent the track superelevation. The equipment used to measure superelevation is shown in Figure 19; the digital level used can provide slope readings down to 0.1 % slope.

**Figure 19. Picture. Straightedge and digital level used for superelevation measurements.**

The manually measured superelevation results can be found in Appendix A. According to the design drawings, the test track was designed to have a 15 % slope on fully superelevated sections of the curves; the manually measured results showed the current test track has a 14-16 % slope on fully superelevated sections.

***Driving Speed and Driving Behavior***

The validation test was performed by making multiple runs of data collection at different driving speeds and with different driving behaviors. Different driving speeds were performed using the vehicle's cruise control system. The test was performed at five different speeds, ranging from 30 MPH to 50 MPH in 5 MPH increments. At each speed, five laps were driven to evaluate the repeatability of the calculation. Different driving behaviors were introduced. For example, the

driver drove as smoothly as possible through the curve to represent “good/optimal” driving behavior; on the last lap, the driver made sudden steering adjustments, which made the vehicle wander over the lane, to mimic “bad/undesired” driving behaviors.

***Data Collection Devices and Setup***


**Figure 20. Picture. Mobile devices used in the validation test and their setup.**

Three mobile devices were used during the validation test, two Android smartphones and a GoPro camera that has internal GPS and IMU sensors. Two smartphones were equipped to evaluate the impact of different mounting methods as Smartphone 1 was mounted with a clamp mount to the dashboard, and Smartphone 2 was mounted with a suction cup that has an extension arm to secure the device. The inclusion of the GoPro camera was to evaluate the impact of the different sensors, as the GPS and IMU sensors in the GoPro camera have a higher sampling frequency than the smartphones; also, the quality of the sensors might be different in the GoPro. In addition, the Rieker inclinometer was included in the test to represent commercial solutions for BBI angle measurement.

### *Test Procedure*

The following procedure was followed to validate the test at NCAT.

**Task 1: Survey the superelevation on the NCAT test track**

1. Using a measuring wheel, locate key reference points (spiral-tangent point and circle-spiral point).
2. Starting from the mid-point of each curve, measure the superelevation at the following distance away from the mid-point.
    a. Distance to mid-point where superelevation is measured:

       0 ft, 200 ft, 400 ft, 543.7 ft, 600 ft, 700 ft, 800 ft, 900 ft, 951.7 ft, 1000 ft, and 1100 ft.
3. At each location, measure superelevation three times with each measurement spaced 1 ft apart. Report the average of the three measurements.

**Task 2: Collect mobile data (in motion)**

1. Set up the data collection devices in the vehicle (Chevy Tahoe SUV).
2. Before the start of each data collection, park the vehicle on the tangent section, preferably riding the centerline to balance the cross-slope.
3. All test devices will start the recording at the same time.
4. After recording starts, stand by for at least 10 seconds for zeroing the BBI measurements.
5. Proceed with the following data collection runs in Table 2. Restart the recording after each run.

**Table 2. Description of the data collection runs.**

| Run Number | Speed (MPH) | Number of Laps (Good Driving + Bad Driving) |
|---|---|---|
| Run 1 | 30 | 4 + 1 |
| Run 2 | 35 | 4 + 1 |
| Run 3 | 40 | 4 + 1 |
| Run 4 | 45 | 4 + 1 |
| Run 5 | 50 | 4 + 1 |
| Total | | 20 + 5 |

### Validation Test Results – Curve Radius Calculation

The NCAT test track has two main curves (West Curve and East Curve) that have the same curve radius. To validate the proposed method for computing curve radius, the estimated curve radius is compared to the curve radius in the design drawings.

#### *NCAT Test Track Centerline*

As mentioned in Chapter 3, the proposed method recommends the use of the roadway centerline for extracting the curve radius. For this test, Google Earth was used to extract the centerline of the test track. Using the "add path" tool, the centerline of the test track was manually traced on the satellite map (using the pavement marking as reference). Figure 21 shows the manually traced centerline overlaid on the satellite map.

**Figure 21. Map. Manually traced centerline (green) on Google Earth.**

### *Curve Radius Calculation*

After obtaining the centerline, the curve radius was computed by using the curve sections on the roadway centerline and using the Kasafit method to estimate the least square fit circle for radius estimation. The estimated curve radius using the proposed method showed a circular radius of 478.1 ft for the West Curve and 481.4 ft for the East Curve. The curve radius documented in the design drawing has a radius of 476 ft for the circular section of the curves. This shows that using the proposed method can very reasonably estimate the curve radius using the roadway centerline.

## Validation Test Results – Superelevation Calculation without Body Roll Calibration

As shown in Equation (11), the superelevation calculations use the driving speed, path radius, and vehicle roll rate. However, the roll rate of the vehicle may not be readily available. In the case of unavailable roll rate information, the superelevation can be approximated by assuming the body roll is small enough that the roll rate constant is equal to zero. This assumption may be reasonable for low travel speeds; however, as/if a vehicle travels faster on curves, the amount of body roll increases; this could cause the assumption to be less accurate than the actual condition. This section presents the accuracy level of superelevation calculation at different driving speeds; it assumes there is no vehicle body roll.

### *Superelevation Results at Different Driving Speeds*

Figure 22 shows the error of uncalibrated superelevation results that were calculated from the three data collection devices. As shown in the charts, at any given speed, the variation in the error (amount of vertical spread) remained similar for all devices, while the results from the GoPro showed the random error is lower in GoPro than in the smartphones. In addition, the bias of the superelevation error has a downward trend with increasing speed. This indicates that, without calibration, the calculation tends to underestimate the superelevation of the roadway

when the vehicle is traveling at high speed. The amount of underestimation has a positive relationship to the travel speed. This behavior is expected and can be explained by Equation (11). When assuming no vehicle body roll, the large BBI angle (typically from higher driving speed) will cause the superelevation results to be lowered.

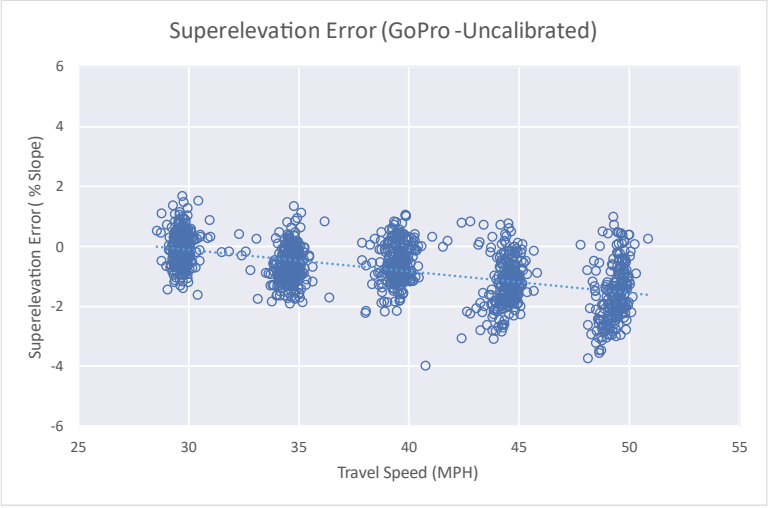


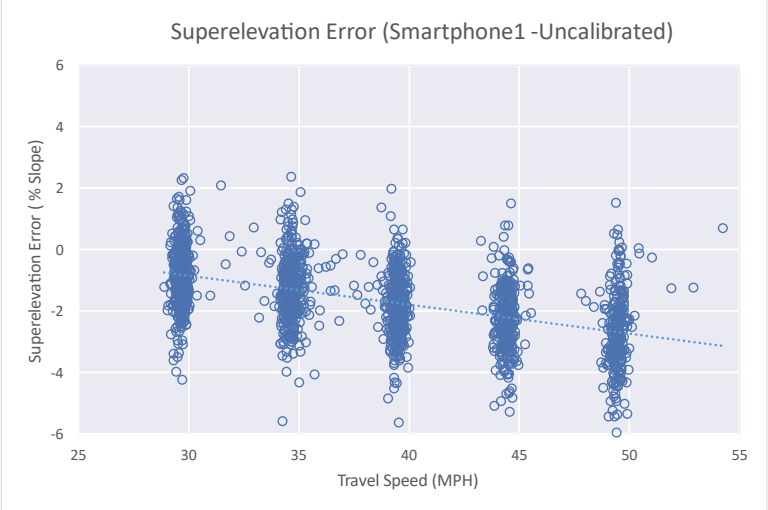

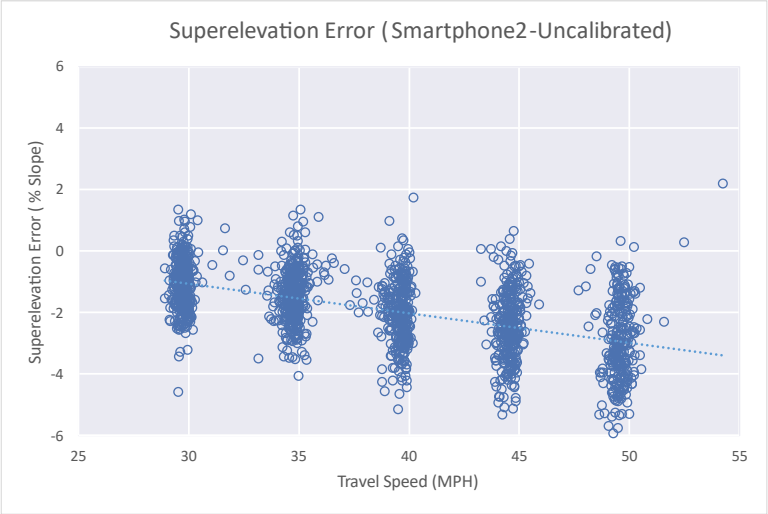


**Figure 22. Charts. Uncalibrated superelevation error at different speeds.**

Table 3 summarizes the root-mean-square error (RMSE) of the uncalibrated superelevation results categorized by vehicle speed, mobile device, and driving behavior. The superelevation RMSE is plotted in Figure 23. The results show that the GoPro data will produce more accurate results than those from the smartphones. Smartphone 1 is slightly more accurate than Smartphone 2, which shows that the mounting mechanism for Smartphone 1 (mounted with dashboard clamp) may improve the accuracy but only slightly. Finally, poor curve driving (shown in Figure 24) does reduce the accuracy of the superelevation calculation. However, with the proposed method, the superelevation error level will only increase by less than 0.5 % slope.

**Table 3. RMSE of uncalibrated superelevation results.**

| | RMSE of Superelevation (GoPro) | | RMSE of Superelevation (Smartphone 1) | | RMSE of Superelevation (Smartphone 2) | |
|---|---|---|---|---|---|---|
| Driving Style | Good | Bad | Good | Bad | Good | Bad |
| 30 MPH | 0.525 | 0.872 | 1.216 | 1.401 | 1.255 | 1.524 |
| 35 MPH | 0.808 | 1.244 | 1.611 | 1.929 | 1.578 | 1.850 |
| 40 MPH | 0.839 | 1.205 | 1.999 | 2.334 | 2.189 | 2.575 |
| 45 MPH | 1.476 | 1.683 | 2.423 | 2.590 | 2.695 | 2.668 |
| 50 MPH | 1.817 | 2.474 | 2.965 | 3.372 | 3.266 | 3.948 |
| **Overall** | **1.093** | **1.496** | **2.043** | **2.325** | **2.197** | **2.513** |

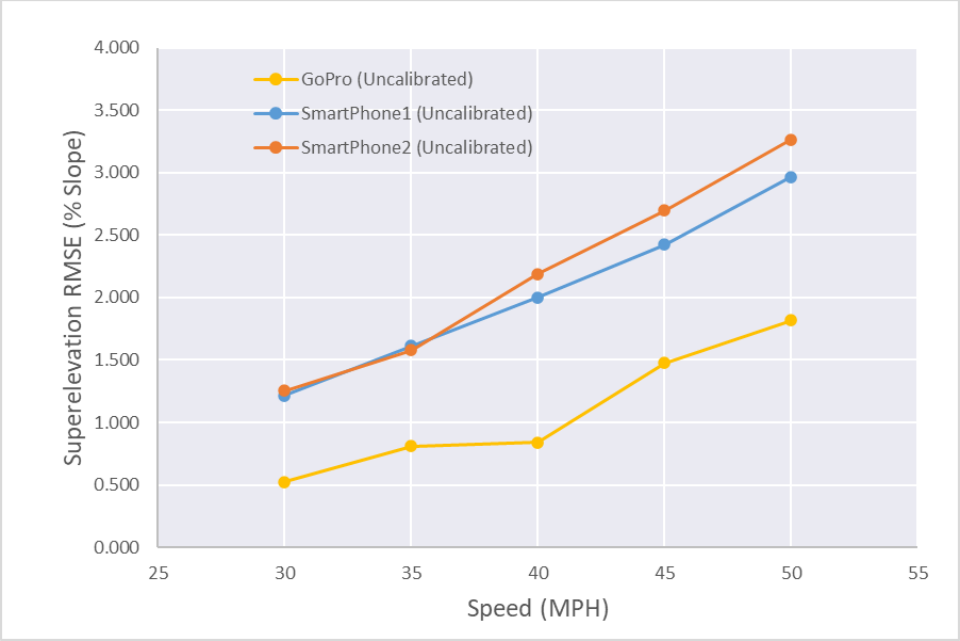


**Figure 23. Chart. RMSE of uncalibrated superelevation.**

### *Importance of Using Path Radius for Superelevation Calculation*

As discussed in the validation test design, the validation test also introduced different driving behaviors to evaluate the robustness of the proposed method. Figure 24 illustrates the different driving behaviors used during the validation test.

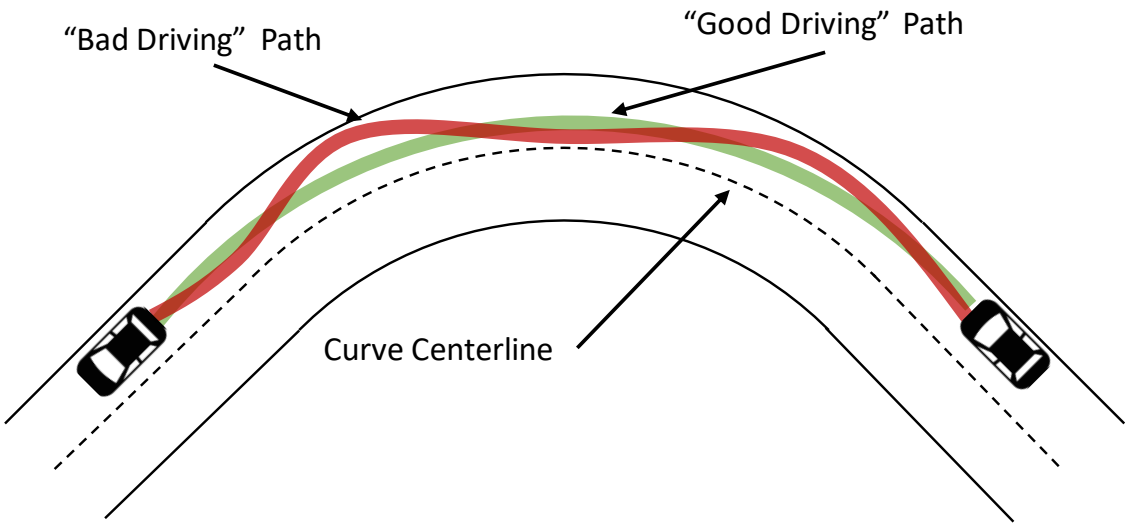


**Figure 24. Diagram. Driving path of different driving behaviors.**

For superelevation calculation, the radius of the vehicle's path is needed, and, generally, the curve's centerline radius is a good approximation of the path radius. As shown in Figure 24, the curvature of the "good driving" path is, generally, similar to the curvature of the centerline. However, some driving behaviors, such as frequent wandering within the lane and "jerking" the wheel when turning, may cause the curvature of the driving path to be drastically different from the centerline. Therefore, at any point during cornering, the superelevation calculation at that point should use the speed, BBI angle, and path radius corresponding to the vehicle at that moment.

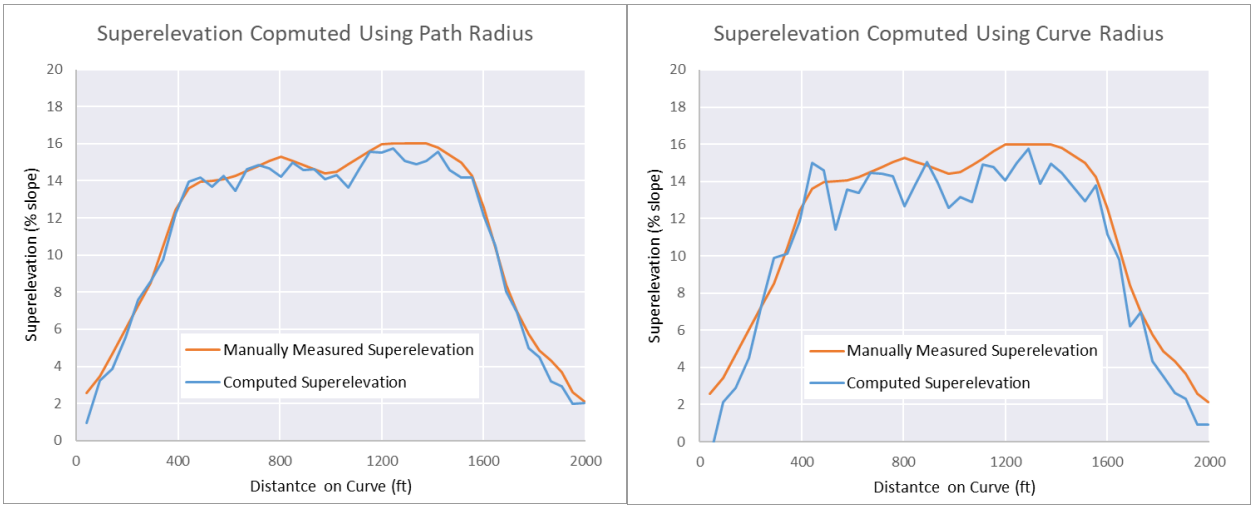


**Figure 25. Charts. Computed superelevation using path radius vs. curve radius in "good driving" cases.**

The example in Figure 25 shows that in "good driving" cases, using the curve radius to approximate the path radius can still result in acceptable superelevation estimation. However, when "bad driving," such as wheel jerking and wandering occurs, the curve radius can no longer describe the vehicle's driving path, leading to significant error in superelevation estimation (shown in Figure 26).

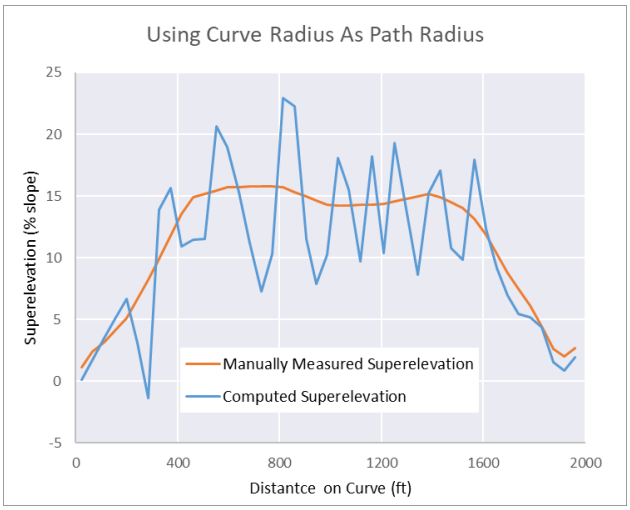


**Figure 26. Chart. Using curve radius as path radius in "bad driving" cases**

***Performance Comparison of Different Path Radius Calculation Methods***

It would be logical for the GPS that captures the vehicle's trajectory to be used to compute the path radius. However, given the GPS sampling rate in smartphones (typically 1 Hz) and the accuracy of GPS (typically about 15 ft), the subtle movement caused by steering input may not be able to be captured. In order to get the path radius at a particular GPS point, the neighboring points are also needed for the least square fitting; therefore, the path radius computed from the GPS cannot represent the curvature of the path at an instant, but the averaged curvature over a small period.

With this in mind, the proposed method measures the path radius from the angular velocity and vehicle speed. The computation for this approach is shown in Chapter 3. Figure 27 shows an example of a "bad driving" case in which the difference in superelevation measurement performance between using the path radius estimated from GPS and using the path radius estimated from the gyroscope.

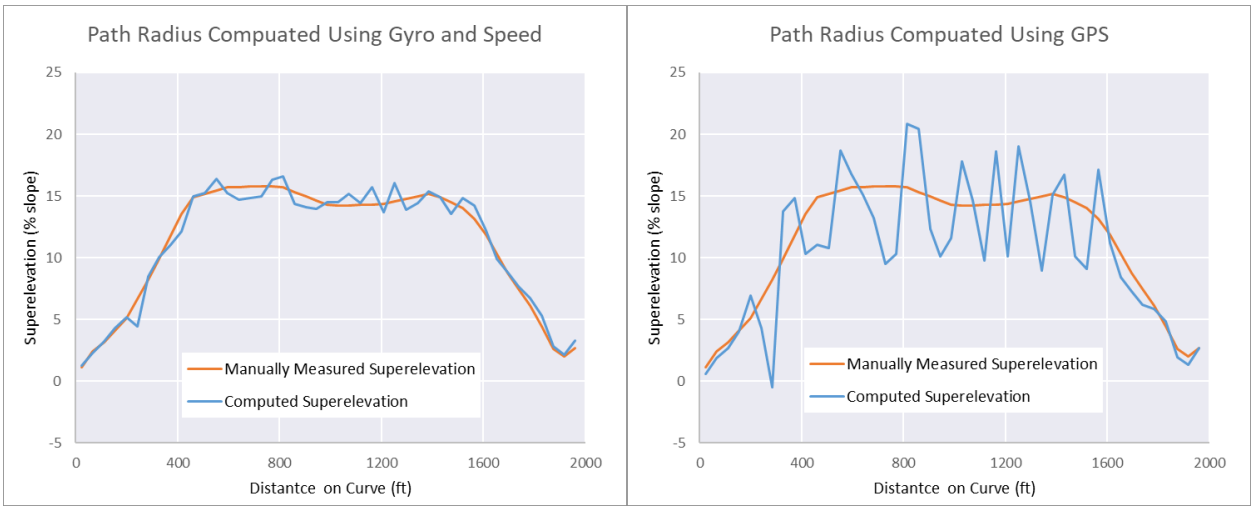


**Figure 27. Charts. The performance difference between different methods of path radius estimation**

From the results, we can see that there is still a significant amount of error in the GPS method. In the case of calculating the path radius from the gyroscope and vehicle speed, the curvature at every point of the cornering process, the radius was captured accurately, leading to no significant performance difference compared to the "good driving" cases.

### Validation Test Results – Vehicle Roll Rate Estimation

As seen in the uncalibrated superelevation results, the vehicle speed has an impact on the accuracy results, as higher speed will introduce more vehicle body roll thus making the results less accurate. The errors introduced may be minimized if the vehicle roll rate is available. However, most vehicle owners do not know their vehicle's roll rate; the roll rate needs to be measured in order to calibrate the superelevation results.

As the proposed methods to estimate vehicle roll rate from collected mobile data are presented in Chapter 3, this section presents the results of the proposed methods using data collected during the NCAT test.

**Table 4. Roll-rate estimation of the data collection vehicle**

| | Estimated Vehicle Roll Rate (rad/rad) | | | | |
|---|---|---|---|---|---|
| **Estimation Method** | **GoPro** | **Smartphone 1** | **Smartphone 2** | **Average Roll Rate** | **Standard Deviation** |
| **With Known Superelevation** | 0.0918 | 0.0958 | 0.1089 | 0.0988 | 0.0073 |
| **With Unknown Superelevation** | 0.0938 | 0.1019 | 0.1202 | 0.1053 | 0.0110 |

***Roll Rate Estimation with Known Superelevation***

As mentioned in Chapter 3, this method uses the measured superelevation to compute the side-friction angle during data collection, and by comparing the relationship between the side-friction angle and the measured BBI angle (shown in Figure 28) to estimate the roll rate of the vehicle.

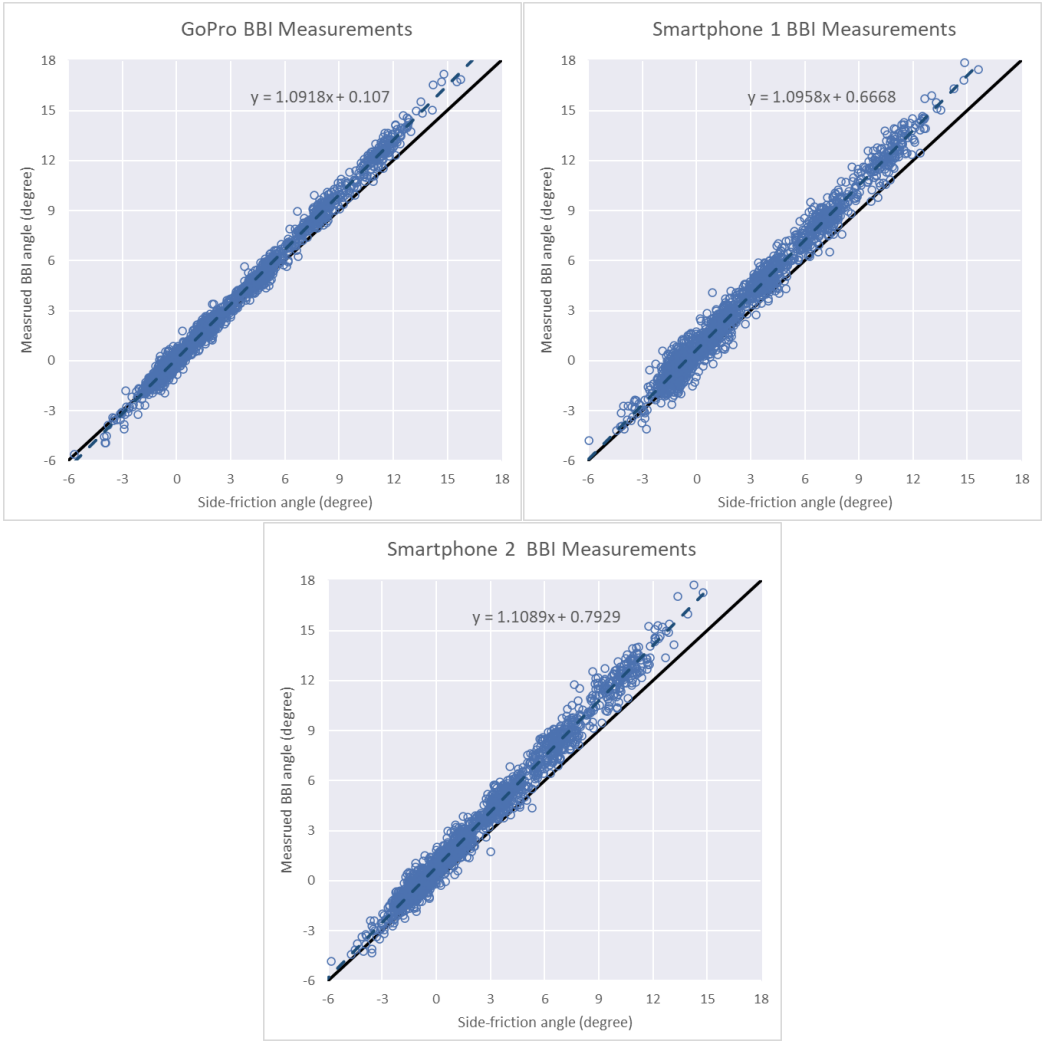


**Figure 28. Charts. Relationship between measured BBI angle and side-friction angle.**

While the true vehicle roll rate is unknown for the data collection vehicle, since all data collection was performed using the same vehicle, the estimated vehicle roll rate using different devices should not be drastically different. Table 4 shows use of the proposed roll rate estimation method with the manually measured superelevation as the known superelevation. The estimated vehicle roll rate from the three-mobile-device test gives similar results, showing an average roll rate of 0.0988 rad/rad and a standard deviation of only 0.0073 rad/rad. This indicates that the proposed "known superelevation" method can estimate roll rate with good repeatability.

***Roll Rate Estimation with Unknown Superelevation***

While the benefit of the roll rate estimation with the known superelevation is simple in its computation, detailed superelevation measurements might not be available in most circumstances. Therefore, as mentioned in Chapter 3, when the superelevation is not available, an alternative approach is to use the vehicle to collect mobile data on the same curve with different speeds. Using the data collected at NCAT with five different speeds (30 MPN – 50 MPN), and with two out of five laps, the vehicle's roll rate was estimated without using the measured superelevation. The results of the estimations are shown in Table 4, and we can see the estimations are also similar between different devices, there is a slight increase in the standard deviation compared to the "known superelevation" method.

Although this approach for estimating the vehicle roll rate requires multiple runs of data collection at different speeds, this approach might be more practical to implement since it does not require any knowledge of the curve geometry, and the repeatability of this method is similar to the "known superelevation" method.

**Table 5. Estimated roll rate with different data collection strategies.**

| | Number of Runs at each speed | Total Number of Runs | Estimated Roll Rate | | |
|---|---|---|---|---|---|
| | | | GoPro | Smartphone 1 | Smartphone 2 |
| Two speeds @ 5 MPH increment | 2 | 4 | 0.1059 | 0.1802 | 0.1593 |
| Two speeds @ 10 MPH increment | 2 | 4 | 0.0984 | 0.1064 | 0.1202 |
| **Two speeds @ 15 MPH increment** | **2** | **4** | **0.1042** | **0.0995** | **0.1085** |
| Two speeds @ 5 MPH increment | 3 | 6 | 0.0858 | 0.1776 | 0.1662 |
| Two speeds @ 10 MPH increment | 3 | 6 | 0.0912 | 0.1170 | 0.1328 |
| **Two speeds @ 15 MPH increment** | **3** | **6** | **0.0946** | **0.1080** | **0.1146** |
| Three speeds @ 5 MPH increment | 2 | 6 | 0.0890 | 0.1186 | 0.1129 |
| **Four speeds @ 5 MPH increment** | **2** | **8** | **0.0925** | **0.1069** | **0.1189** |

To investigate the recommended speed difference between runs and the number of runs at each speed for this roll rate estimation method, Table 5 shows the estimated roll rate using different data collection strategies. We can see that while more runs generally improve the method's repeatability, the speed difference between the highest and lowest data collection speed plays a more important role in the result's repeatability. Therefore, if the method is to be formalized as a calibration method, performing the calibration test at two different speeds and repeating each speed two times should be enough to produce a reasonable roll rate estimation; repeating each speed three times would produce an estimation with higher confidence.

**Validation Test Results – Superelevation Calculation with Body Roll Calibration**

Using the vehicle roll rate estimated by the proposed method, the superelevation results can be calibrated to compensate for the impact of vehicle body roll. Figure 29 shows the comparison of the superelevation error before and after calibration using the estimated vehicle roll rate. Table 6 summarizes the RMSE of the uncalibrated superelevation results and is separated based on

vehicle speed, mobile device, and driving behavior. The superelevation RMSE is plotted in Figure 30. The results show, after calibration, the superelevation measurement accuracy is no longer impacted by the travel speed. It is worth noting the device's random noise level (vertical spread at each speed) is unaffected by the calibration.

The validation results show that after calibration, the GoPro camera is able to measure superelevation with 0.598 % slope accuracy, and the smartphones can achieve a measurement accuracy between 1.4 -1.5 % slope.

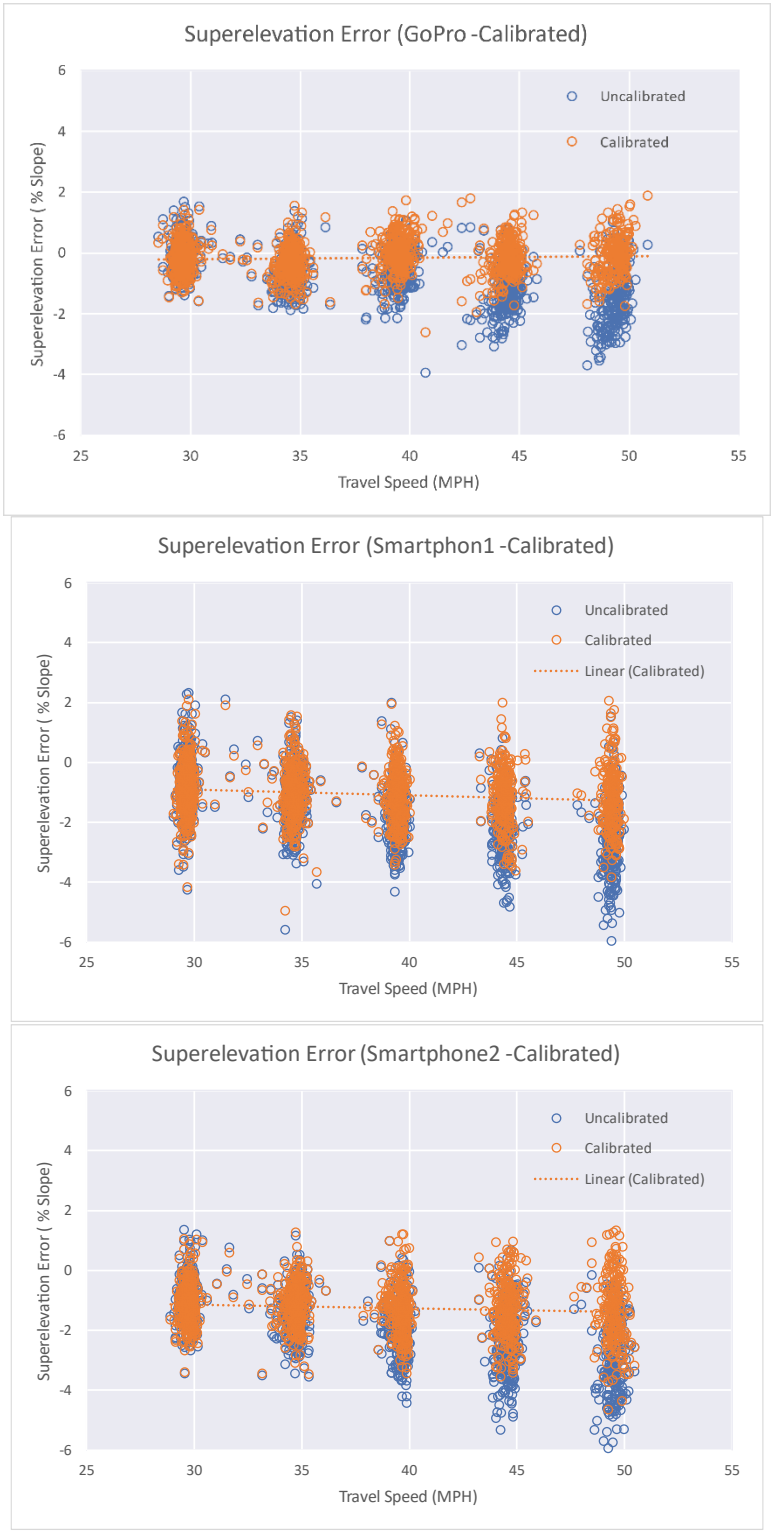


**Figure 29. Charts. Calibrated superelevation error at different speeds.**

**Table 6. RMSE of Calibrated superelevation results.**

| | RMSE of Superelevation (GoPro) | | RMSE of Superelevation (Smartphone 1) | | RMSE of Superelevation (Smartphone 2) | |
|---|---|---|---|---|---|---|
| Driving Style | Good | Bad | Good | Bad | Good | Bad |
| 30 MPH | 0.522 | 0.695 | 1.226 | 1.366 | 1.318 | 1.501 |
| 35 MPH | 0.622 | 0.820 | 1.368 | 1.629 | 1.322 | 1.441 |
| 40 MPH | 0.576 | 0.638 | 1.434 | 1.615 | 1.532 | 1.808 |
| 45 MPH | 0.619 | 0.758 | 1.473 | 1.590 | 1.599 | 1.524 |
| 50 MPH | 0.652 | 1.509 | 1.556 | 2.181 | 1.729 | 2.490 |
| **Overall** | **0.598** | **0.884** | **1.411** | **1.676** | **1.500** | **1.753** |

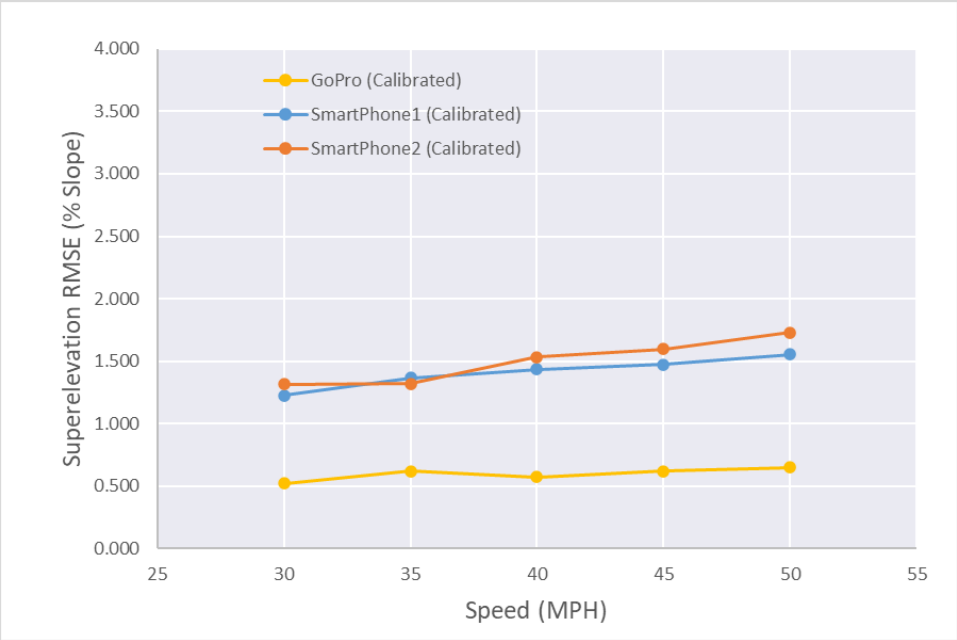


**Figure 30. Chart. RMSE of Calibrated superelevation.**

### Validation Test Results – BBI Angle Computation

In order to assess the BBI angle measurement accuracy, the manually measured superelevation values were used to back-calculate the expected BBI angle base on the side-frication angle and the vehicle's body roll. Table 7 shows the RMSE of the BBI angle measured by each device. And the linear regression between measured and expected BBI angle is shown in Figure 31.

**Table 7. RMSE of measured BBI angles compares to expected BBI angle computed from side-friction angles and vehicle body roll.**

| | GoPro | Smartphone 1 | Smartphone 2 | [1]Rieker Inclinometer |
|---|---|---|---|---|
| BBI RMSE (degree) | 0.390 | 0.901 | 0.964 | 0.519 |

[1]Rieker inclinometer data collected at 30 and 50 MPH was not included due to data corruption.

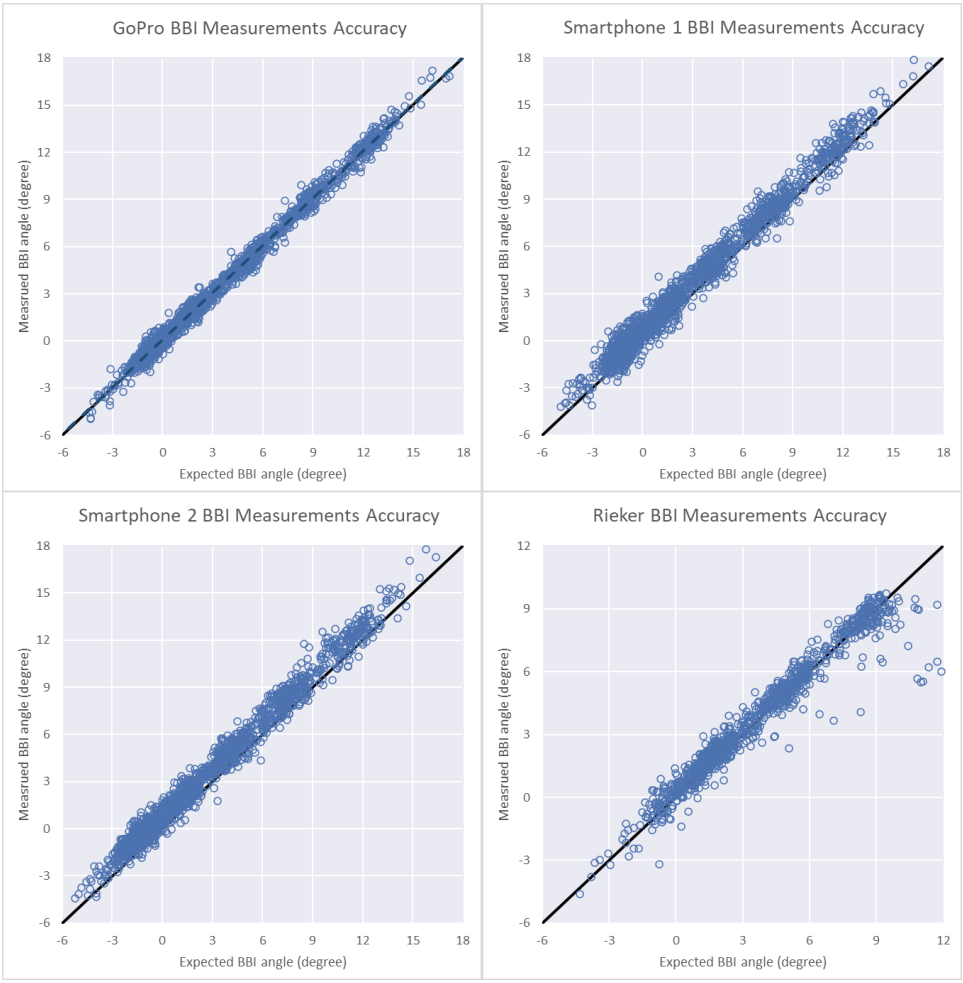


**Figure 31. Charts. Linear regression between BBI angles measured using different device and expected BBI angles.**

It is worth noting that since the expected BBI angle is back-calculated from side-friction angles, the accuracy of the side-friction angle, which is dependent on the measured superelevation, vehicle speed, and path radius estimation, will affect the expected BBI angle. Therefore, the RMSE values presented in the table do not represent the BBI measurement error by itself. However, since the true BBI angle at every moment of data collection is difficult to obtain, the RMSE values presented are a good general indication of the BBI measurement accuracy.

### Validation Test Results – Advisory Speed Computation

Table 8 shows the advisory speed results using the proposed method. From the manually

measured superelevation, the exact advisory speed on the test track curves should be 49.7 MPH. The validation results show that, without calibration, as the superelevation is underestimated, the determined advisory speed decreases as data collection speed increases; however, the advisory speed difference between the lowest data collection speed and the highest data collection is less than 2 MPH.

After calibration, the superelevation is no longer being underestimated at high speed. The advisory speed results are very consistent at different speeds. The variation of the advisory speed across all data collection speeds is less than 1 MPH. Compared to the advisory speed computed from manually measured superelevation, the advisory speed results from the GoPro showed less than 0.5 MPH difference (underestimation), and the smartphones showed less than 1.3 MPH difference (underestimation).

**Table 8. Advisory speed results before and after calibration.**

| **Before Calibration** | | | | | | |
|---|---|---|---|---|---|---|
| | **GoPro** | | **Smartphone 1** | | **Smartphone 2** | |
| **Driving Speed** | **Average Adv. Speed** | **Standard Deviation** | **Average Adv. Speed** | **Standard Deviation** | **Average Adv. Speed** | **Standard Deviation** |
| 30 MPH | 49.618 | 0.197 | 48.545 | 0.285 | 48.791 | 0.323 |
| 35 MPH | 49.266 | 0.231 | 47.986 | 0.748 | 48.692 | 0.181 |
| 40 MPH | 49.066 | 0.333 | 47.870 | 0.070 | 47.890 | 0.237 |
| 45 MPH | 48.339 | 0.404 | 47.674 | 0.320 | 47.591 | 0.408 |
| 50 MPH | 48.095 | 0.408 | 46.892 | 0.431 | 46.690 | 0.393 |
| **Overall** | **48.877** | **0.670** | **47.794** | **0.643** | **47.931** | **0.830** |
| **After Calibration** | | | | | | |
| | **GoPro** | | **Smartphone 1** | | **Smartphone 2** | |
| **Driving Speed** | **Average Adv. Speed** | **Standard Deviation** | **Average Adv. Speed** | **Standard Deviation** | **Average Adv. Speed** | **Standard Deviation** |
| 30 MPH | 49.635 | 0.177 | 48.588 | 0.278 | 48.852 | 0.300 |
| 35 MPH | 49.616 | 0.220 | 48.405 | 0.679 | 49.077 | 0.196 |
| 40 MPH | 49.782 | 0.319 | 48.692 | 0.066 | 48.749 | 0.262 |
| 45 MPH | 49.466 | 0.435 | 48.862 | 0.256 | 48.866 | 0.373 |
| 50 MPH | 49.621 | 0.373 | 48.620 | 0.396 | 48.412 | 0.380 |
| **Overall** | **49.624** | **0.324** | **48.633** | **0.412** | **48.791** | **0.340** |

***Sensitivity of Advisory Speed Results and Tolerance for Computation Error***

Because the curves at the NCAT test track only have one curve geometry, a mathematical

sensitivity study was conducted to determine the tolerance for error for curves with different geometry. Since the advisory speeds are typically rounded down to the closest 5 MPH, the error tolerances presented in Table 9 show the amount of error allowed in each factor that will not change the final computed advisory speed.

**Table 9. Error tolerance for the computed data items**

| Factor | Most Sensitive When… | Error Tolerance | Least Sensitive When… | Error Tolerance |
|---|---|---|---|---|
| BBI angle | Large Radius, Low Speed | 1 degree | Small Radius, High Speed | 6 degrees |
| Superelevation | Large Radius | 3% | Small Radius | 8% |
| Curve Radius | Low BBI, Low Speed | 150 ft | High BBI, High Speed | 350 ft |

As shown in the table, the sensitivity of each factor depends on the curve geometry and data collection characteristics. For accurate results in all cases, the BBI should be precise within 1 degree, the superelevation should be precise within 3%, and the curve radius should be precise within 150 ft. From the validation results presented in this chapter, we can conclude that the accuracy of the computed BBI angle, superelevation, and curve radius is within the error tolerance.

## VALIDATION SUMMARY

The validation test presented in this chapter showed that using vehicle roll rate in superelevation calculation can dramatically reduce the error caused by different data collection speeds. It also shows that the proposed calibration method can estimate the vehicle's roll rate to compensate in superelevation calculation. The superelevation results before calibration showed an overall RMSE of about 1.0 % slope for the GoPro camera, and about 2.0 – 2.2 % slope for the smartphones. The superelevation error before calibration increases as driving speed increases, the superelevation RMSE at 50 MPH for the GoPro camera is about 1.8 % slope, and 3.2 % slope for the smartphones. After calibration, the superelevation error introduced by the driving speed is

almost completely eliminated, resulting in an overall RMSE of about 0.6 % slope for the GoPro camera, and about 1.4 – 1.5 % slope for the smartphones. The BBI angle validation showed the GoPro camera (RMSE = 0.39 degrees) can estimate the BBI angle accurately enough to be comparable to commercial BBI devices (RMSE = 0.52 degrees), while the smartphones have an RMSE of 0.9 – 0.96 degrees, slightly worse than commercial devices but accurate enough for advisory speed determination. Finally, the advisory speed results show that the determined advisory speeds are very close to the advisory speed computed using measured superelevation, having a difference of less than 3 MPH before calibration and about 1 MPH after calibration.

# CHAPTER 5. CASE STUDY

This section presents a preliminary case study using five runs of smart phone data collected on Georgia State Route 17 in September 2020, November 2020, and March 2021. The case study demonstrates the use of the proposed method using smart phones to perform curve safety assessment. The purpose of this case study is to demonstrate the feasibility of using the proposed method to derive the curve radius, BBI, superelevation, and advisory speed using smart phones. Furthermore, the case study provides an assessment of the confidence level of the outcomes. In addition, the smartphone and Rieker device were both mounted in the same vehicle, simultaneously to collect data for comparison. This is to compare the outcomes derived using the proposed method to those of the current, commonly used current assessment method, which uses dedicated Rieker devices.

## FEASIBILITY STUDY OF THE PROPOSED METHODOLOGY USING SMART PHONE DATA COLLECTED ON GEORGIA STATE ROUTE 17

The purpose of this case study is to assess and demonstrate the feasibility of using the proposed method to derive the curve radius, BBI, superelevation, and advisory speed using smart phones and the smart phone data collected on Georgia State Route (SR) 17.

### Data Collection

After discussing the best locations to test the proposed system with traffic engineers in the Georgia Department of Transportation (GDOT), SR 17 was chosen as the best location on which to perform this feasibility study because of the curvy nature of SR 17 and the frequency of crashes on the road. Figure 32 shows a map of the SR 17 test sites chosen for data collection with a close view of five curve sections that were used for the detailed data processing and analysis in

our feasibility study. The selected portion of SR 17 is a two-lane, undivided rural minor arterial road with occasional painted/striped medians. This portion of SR 17 is mountainous and has many curves.

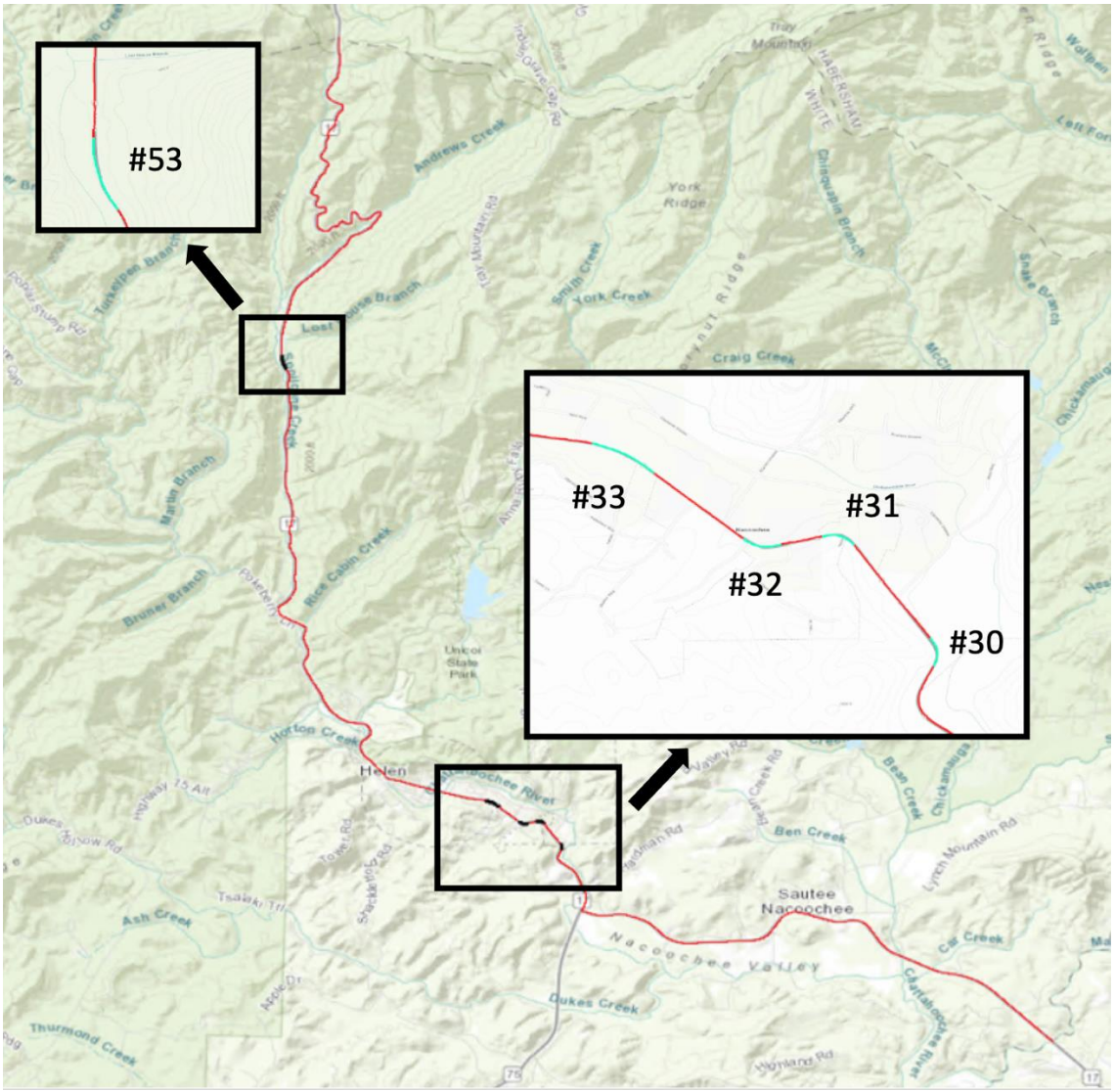


**Figure 32. Map. State Route 17 in Georgia (mountain area) and selected curves.**

The field data collection using smartphones was conducted with five runs in each direction. Data collection was carried out September 23, 2020, with GDOT Ford F150; November 11, 2020, with a Ford Fusion; November 4, 2020, with a GDOT Ford F150; November 6, 2020, using a

GDOT Ford F150; and March 25, 2021, with GDOT Ford F150. Five runs in each direction were made in sunny weather conditions on each date. Each vehicle was equipped with one smartphone for data collection. Figure 33(a) shows the GDOT truck. Figure 33(b) shows a smartphone used for testing. The phone is a regular Android smartphone. The smartphone data collected includes 1) timestamp, 2) speed, 3) GPS data, and 4) IMU data.

A. Subfigure showing the GDOT truck used for data collection

B. Subfigure showing the smart phone used for data collection

**Figure 33. Photos. GDOT truck and smartphone used for field data collection.**

**Data Processing**

The collected smart phone data, including timestamp, speed, GPS data, and IMU data, were processed for each of the five single runs, respectively. Since the detailed description on the data processing is provided in the proposed method and validation sections, it will not be duplicated in this section. The subsequent section presents the data analysis.

**Data Analysis**

The data collected using the smart phones were processed to find the curve radius, BBI, superelevation, and advisory speed at each point. Using the five runs of data, it is possible to also assess the inherent variability of the outcomes using smart phone data. Table 10 presents the location and geometry of the five curves tested. Table 11 shows the range of radius, BBI, superelevation, and computed advisory speed for each curve. The BBI and superelevation values

refer to those at the point of minimum computed advisory speed.

**Table 10. Characteristics of the five curves tested on SR 17.**

| Curve ID | Latitude | Longitude | Radius (ft) | Length (ft) |
|---|---|---|---|---|
| 30 | 34.69346272 | -83.71341549 | 287 | 386 |
| 31 | 34.69683579 | -83.71588127 | 222 | 320 |
| 32 | 34.69679324 | -83.71802552 | 350 | 430 |
| 33 | 34.69904781 | -83.72191988 | 1135 | 733 |
| 53 | 34.75750134 | -83.75033975 | 921 | 575 |

**Table 11. Variability of curve characteristics estimated using smartphone.**

| Northbound | | | | | | |
|---|---|---|---|---|---|---|
| **Curve ID** | **Radius (ft)** | **BBI (degrees)** | **Superelevation (%)** | **Advisory Speed (mph)** | **Posted Speed Limit (mph)** | **Final Advisory Speed (mph)** |
| 30 | 192 – 239 | 0.10 – 5.70 | 2.72 – 5.49 | 32.13 – 33.94 | 55 | 30 |
| 31 | 181 – 192 | 0.16 – 1.68 | 4.79 – 7.52 | 29.44 – 30.94 | 55 | 30 |
| 32 | 255 – 280 | 2.86 – 12.98 | 0.05 – 1.55 | 33.46 – 33.75 | 55 | 30 |
| 33 | 844 – 981 | 0.23 – 1.45 | 3.73 – 5.52 | 65.22 – 66.64 | 55 | none |
| 53 | 563 – 780 | 0.23 – 3.97 | 0.15 – 4.74 | 54.40 – 59.95 | 55 | none |
| **Southbound** | | | | | | |
| **Curve ID** | **Radius (ft)** | **BBI (degrees)** | **Superelevation (%)** | **Advisory Speed (mph)** | **Posted Speed Limit (mph)** | **Final Advisory Speed (mph)** |
| 30 | 192 – 229 | 3.51 – 7.14 | 0.57 – 2.47 | 30.66 – 31.96 | 55 | 30 |
| 31 | 154 – 199 | 1.81 – 5.84 | 1.92 – 6.78 | 27.77 – 30.54 | 55 | 30 |
| 32 | 280 – 317 | 0.71 – 4.56 | 0.01 – 11.10 | 33.42 – 35.03 | 55 | 35 |
| 33 | 812 – 975 | 0.32 – 1.61 | 2.57 – 5.72 | 62.16 – 67.76 | 55 | none |
| 53 | 650 – 826 | 2.76 – 6.88 | 0.17 – 0.80 | 54.42 – 55.22 | 55 | none |

Using five sample curves on SR 17, it was found that the average variability of measurements between runs of the data collection is approximately 49 feet for the radius, 8 degrees for the BBI, 5% for the superelevation, and 2 mph for the computed advisory speed. Table 11 and Table 12 list the range of the estimated radius, measured BBI, estimated superelevation, and computed advisory speed values of the five runs of data for the five selected curves in the Northbound and Southbound directions, respectively. The results show that there is a high level of consistency in the advisory speed computation among the five runs of smart phone data, which means there is a

high confidence in the outcomes.

For the advisory speed computation, the standard practice is to add 1 and then round down the raw computed result to the nearest multiple of 5 for advisory speed plaque design. If all runs of the data collection yield the same rounded computed advisory speed, it indicates a very high confidence in that result. For the five sample curves studied on SR 17, each curve had ten total passes of smart phone data collection, five in each direction. The number of passes from each curve yielding the same advisory speed are shown in Table 12.

**Table 12. Consistency of computed advisory speed from multiple runs.**

| Curve ID | Direction | Design Advisory Speed | Runs in Agreement |
|---|---|---|---|
| 30 | Northbound | 30 mph | 5/5 |
| | Southbound | 30 mph | 5/5 |
| 31 | Northbound | 30 mph | 5/5 |
| | Southbound | 30 mph | 4/5 |
| 32 | Northbound | 30 mph | 5/5 |
| | Southbound | 30 mph | 4/5 |
| 33 | Northbound | 65 mph | 5/5 |
| | Southbound | 65 mph | 4/5 |
| 53 | Northbound | 55 mph | 4/5 |
| | Southbound | 55 mph | 5/5 |

This demonstrates a high level of repeatability in the outcomes of the proposed method using smart phones. It should be noted that due to the nature of the advisory speed rounding, two computations that are very close could give different advisory speeds (e.g., 29 would be rounded to 30 mph while 28 would be rounded to 25 mph). So, some variation in the final computed advisory speed is acceptable. If a curve has more than 5 mph of variation between the computed advisory speeds from different runs, the result is significantly different enough that the data should be re-collected. In choosing the appropriate advisory speed for a curve, the highest computed advisory speed from the multiple runs should be selected because the highest computed advisory speed will be the closest to the true roadway conditions. The computation can

be skewed unnaturally low through erratic driver behavior (changing speeds, jerking the wheel, failing to follow the road trajectory, etc.). On the contrary, there is no way to unnaturally increase the computed advisory speed through human error, so the highest result should most closely estimate the true value. The analysis of five curves on SR 17 demonstrates that the proposed method using smart phone is feasible to compute the curve radius, BBI, superelevation, and advisory speed.

## COMPARISON OF OUTCOMES USING THE PROPOSED METHOD USING SMART PHONES AND THE METHOD USING RIEKER DEVICES

As most transportation agencies are currently using the method that uses dedicated Rieker devices, the research project compares the outcomes of the proposed method (that uses smart phones) and the current commonly used method (that uses dedicated Rieker devices). One vehicle, equipped with both a smart phone and a RIEKER device, collected data on March 11, 2021, for comparing the performance between the proposed method and the method with RIEKER devices.

Table 13 below compare the computed advisory speed output from each method. As shown, for these five sample curves, the proposed method and the Rieker method produce results within 6 mph of one another. Thus, these two methods are comparable.

**Table 13. Computed advisory speed comparison.**

| Northbound | | | |
|---|---|---|---|
| **Curve ID** | **Source** | **Advisory Speed (mph)** | **Posted Speed Limit (mph)** |
| 30 | Smart Phone | 32.7 | 55 |
| | Rieker | 30.4 | 55 |
| 31 | Smart Phone | 30.5 | 55 |
| | Rieker | 25.9 | 55 |
| 32 | Smart Phone | 33.5 | 55 |
| | Rieker | 34.5 | 55 |
| 33 | Smart Phone | 65.7 | 55 |
| | Rieker | 60.1 | 55 |
| 53 | Smart Phone | 55.3 | 55 |
| | Rieker | 56.9 | 55 |
| **Southbound** | | | |
| **Curve ID** | **Source** | **Advisory Speed (mph)** | **Posted Speed Limit (mph)** |
| 30 | Smart Phone | 32.0 | 55 |
| | Rieker | 30.8 | 55 |
| 31 | Smart Phone | 30.5 | 55 |
| | Rieker | 29.2 | 55 |
| 32 | Smart Phone | 33.9 | 55 |
| | Rieker | 34.0 | 55 |
| 33 | Smart Phone | 67.8 | 55 |
| | Rieker | 64.1 | 55 |
| 53 | Smart Phone | 54.4 | 55 |
| | Rieker | 50.2 | 55 |

The smart phone data and Rieker data can also be compared in terms of repeatability. Repeatability of the computed advisory speed is important because it determines the overall confidence in the outcome. For the aforementioned five sample curves, the standard deviation of the computed advisory speed between the multiple runs of data collection was computed. It was found that the standard deviation of the computed advisory speed derived from the smart phone data is 0.89 mph, and the standard deviation of the computed advisory speed derived from the Rieker data is 1.59 mph. Thus, the advisory speed computation using the smart phone method is nearly twice as consistent.

## CASE STUDY SUMMARY

This chapter demonstrates the feasibility of implementation of the proposed method using smart phone data to perform curve safety assessment. This is shown through a case study of five curves on State Route 17 with five runs of data collection each. The results are also compared to the outcomes from the commonly used Rieker data. The preliminary case study shows that the proposed method, using smart phone, has promising results with comparable outcomes to Rieker's method. A large dataset with diverse curve characteristics is recommended for future research. It should also be noted that the new calibration procedure has not been applied to the smart phone data used in this case study, so the accuracy can be further improved once the new calibration procedure is incorporated.

# CHATPER 6. CONCLUSIONS AND RECOMMENDATIONS

The objectives of this research project are to develop an enhanced curve safety assessment method that uses low-cost mobile devices and new proposed computation methods and to critically assess the feasibility of the proposed method for network level curve safety condition assessment. The following are the conclusions for this research project.

1) A method using low-cost mobile devices and a new intra-agency, crowdsourced data collection and computational framework has been developed to assist transportation agencies cost effectively and safely collect curve characteristics and assess network-level curve safety conditions. The proposed data collection and computational framework consists of six modules, and the key data items computed using the proposed method include BBI angles, curve radius, superelevation, and advisory speed.

2) The proposed method uses a vehicle's roll rate for more accurate superelevation calculations. In addition, two calibration procedures were proposed to estimate the vehicle's roll rate. The proposed calibration can be done by simply collecting mobile data on curves with known superelevation or collecting multiple runs of data on the same curve at different speeds, without the need to manually measure true superelevation.

3) A data collection application "AllGather" was built for Android smartphones. "All Gather" is an advanced dashcam-like application that collects a driving video log, GPS data, IMU data, and driving speed.

4) The proposed method has been validated using the data collected on 1.7 miles of the NCAT test track to evaluate the feasibility of using the proposed method to compute curve safety assessment-related data items using the data collected from mobile devices.

Results show that the proposed method can achieve accurate results for computing superelevation, curve radius, BBI angle, and curve advisory speed.

a) The validation test showed that, using typical smartphones for data collection, the results of superelevation, without calibration to compensate for vehicle body roll, the superelevation measurement the accuracy continuously decrease with increasing speed, up to an RMSE of 3.2 % slope at high speed, which results in a 3 MPH difference in the determined advisory speed. With calibration using the proposed method, the superelevation results from smartphones can consistently achieve an RMSE of 1.4 – 1.5 % slope at different data collection speed, and the advisory speed result is about 1 MPH off from the advisory determined from the manually measured superelevation.

b) The proposed method recommends the use of the curve centerline for curve radius estimation. The validation test shows that with a good quality centerline, the estimated curve radius is very close to the curve radius from the curve design drawings.

c) A sensitivity study conducted reveals that, since the advisory speed is typically rounded down to the nearest 5 MPH, the accuracy level of the data items computed will result in the determined advisory speed to be within the 5 MPH range of the true advisory speed of the curve.

5) A preliminary case study using the proposed method and smartphone data collected on five curves with 5 runs of data collection on Georgia State Route 17 demonstrates it is feasible to compute curve characteristics information using typical smartphones. Using

five curves with five runs of data collected in each driving direction, the results demonstrate that the proposed method shows very little variability; in most cases, the five data collection runs resulted in the same advisory speed (after rounding down to the nearest 5 MPH), and in other cases, four out of five runs result in the same advisory speed. This suggest the advisory speed obtained from the proposed method is highly repeatable. If using the variability between multiple runs of data collection as an indication of the confidence level of the data, this would suggest the results computed from the proposed method have a high confidence level.

The proposed method has been developed, and the preliminary study has shown the outcomes are promising. The following are the recommendations for the future work:

1) It is recommended to further evaluate and refine the proposed method, including the developed data collection application and computation method for implementation, by performing a pilot study to collect the data on the roadways with diverse conditions (curve type, geometry, radius, etc.) and using state DOT-owned vehicles. It is recommended to compare the outcomes with the commonly used method using RIEKER devices.

2) It is recommended to explore the implementation of the proposed method in state DOTs' business operations dealing with network-level curve safety assessment and analysis, and the establishment of advisory speeds on curves.

3) It is recommended to include local transportation agencies (counties and cities) in the pilot study because local transportation agencies have limited resources; it would be very helpful to them in improving their roadway safety assessment to be able to use the proposed method and low-cost data collection devices.

4) It is recommended to further evaluate the cost, performance, and practicality of other types of mobile devices for data collection.

5) It is recommended that the proposed calibration method for estimating a vehicle's roll rate be further researched using the mechanically measured roll rate as the ground reference; also, further study should be performed to enhance the accuracy of the proposed estimation method and the impact of estimation errors.

# APPENDIX A. MANUAL SUPERELEVATION MEASUREMENTS ON THE NCAT TEST TRACK

| East Curve – North Part | | | | | | |
|---|---|---|---|---|---|---|
| Location | Distance from Mid-point (ft) | Track Station (ft) | Superelevation Measurement #1 | Superelevation Measurement #2 | Superelevation Measurement #3 | Average Measurement |
| Mid-Point | 0 | 110+00.00 | 14.2 | 14.4 | 14.1 | 14.2 |
| | 200 | 112+00.00 | 14.2 | 14.6 | 14.2 | 14.3 |
| | 400 | 114+00.00 | 15.6 | 14.9 | 15.1 | 15.2 |
| CS Point | 543.7 | 115+43.70 | 13.8 | 13.8 | 13.8 | 13.8 |
| | 600 | 116+00.00 | 12.0 | 12.4 | 12.2 | 12.2 |
| | 700 | 117+00.00 | 8.6 | 8.6 | 8.6 | 8.6 |
| | 800 | 118+00.00 | 5.7 | 5.6 | 5.6 | 5.6 |
| | 900 | 119+00.00 | 1.7 | 1.7 | 1.5 | 1.6 |
| ST Point | 951.7 | 119+51.70 | 2.8 | 2.7 | 2.7 | 2.7 |
| Tangent | 1000 | 120+00.00 | 2.8 | 2.5 | 2.7 | 2.7 |
| Tangent | 1100 | 121+00.00 | 2.2 | 2.0 | 2.0 | 2.1 |
| **East Curve – South Part** | | | | | | |
| Location | Distance from Mid-point (ft) | Track Station (ft) | Superelevation Measurement #1 | Superelevation Measurement #2 | Superelevation Measurement #3 | Average Measurement |
| | 200 | 12+00.00 | 15.8 | 15.7 | 15.9 | 15.8 |
| | 400 | 14+00.00 | 15.6 | 15.6 | 15.8 | 15.7 |
| CS Point | 543.7 | 15+43.70 | 14.7 | 15.0 | 14.9 | 14.9 |
| | 600 | 16+00.00 | 13.1 | 13.0 | 12.9 | 13.0 |
| | 700 | 17+00.00 | 8.6 | 8.8 | 8.7 | 8.7 |
| | 800 | 18+00.00 | 5.1 | 5.1 | 5.1 | 5.1 |
| | 900 | 19+00.00 | 3.0 | 2.6 | 3.0 | 2.9 |
| ST Point | 951.7 | 19+51.70 | 2.1 | 2.3 | 1.9 | 2.1 |
| Tangent | 1000 | 20+00.00 | 0.0 | 0.0 | 0.1 | 0.0 |
| Tangent | 1100 | 21+00.00 | 2.6 | 2.6 | 2.7 | 2.6 |
| **West Curve – North Part** | | | | | | |
| Location | Distance from Mid-point (ft) | Track Station (ft) | Superelevation Measurement #1 | Superelevation Measurement #2 | Superelevation Measurement #3 | Average Measurement |
| Mid-Point | 0 | 155+03.41 | 14.3 | 14.4 | 14.2 | 14.3 |
| | 200 | 153+03.41 | 15.1 | 15.4 | 15.3 | 15.3 |
| | 400 | 151+03.41 | 14.1 | 14.1 | 14.2 | 14.1 |
| CS Point | 543.7 | 149+59.71 | 13.9 | 13.9 | 13.8 | 13.9 |
| | 600 | 149+03.41 | 12.7 | 12.9 | 12.7 | 12.8 |
| | 700 | 148+03.41 | 8.7 | 8.7 | 8.8 | 8.7 |
| | 800 | 147+03.41 | 6.2 | 6.2 | 6.2 | 6.2 |
| | 900 | 146+03.41 | 3.4 | 3.6 | 3.8 | 3.6 |
| ST Point | 951.7 | 145+51.71 | 2.8 | 2.7 | 2.7 | 2.7 |
| Tangent | 1000 | 145+03.41 | 1.8 | 1.9 | 1.8 | 2.0 |
| Tangent | 1100 | 144+03.41 | 2.2 | 2.3 | 2.1 | 2.2 |
| **West Curve – South Part** | | | | | | |
| Location | Distance from Mid-point (ft) | Track Station (ft) | Superelevation Measurement #1 | Superelevation Measurement #2 | Superelevation Measurement #3 | Average Measurement |
| | 200 | 53+03.41 | 16.0 | 15.9 | 16.1 | 16.0 |
| | 400 | 51+03.41 | 15.8 | 16.1 | 16.1 | 16.0 |
| CS Point | 543.7 | 49+59.71 | 14.8 | 14.7 | 14.5 | 14.7 |
| | 600 | 49+03.41 | 12.6 | 12.6 | 12.7 | 12.6 |
| | 700 | 48+03.41 | 8.0 | 7.9 | 7.9 | 7.9 |
| | 800 | 47+03.41 | 5.1 | 5.1 | 5.0 | 5.1 |
| | 900 | 46+03.41 | 3.8 | 4.0 | 4.0 | 3.9 |
| ST Point | 951.7 | 45+51.71 | 2.7 | 2.3 | 2.9 | 2.6 |
| Tangent | 1000 | 45+03.41 | 2.0 | 2.1 | 2.1 | 2.1 |
| Tangent | 1100 | 44+03.41 | 2.0 | 2.0 | 2.1 | 2.0 |

CS = Curve to Spiral

ST = Spiral to Tangent

# ACKNOWLEDGEMENT

This research project is sponsored by NCHRP and cost-shared with GDOT with the Research Project 19-17. The authors would like to thank the support from the NCHRP, especially Dr. Inam Jawed, and the support from GDOT, especially Ms. Meg Pirkle, Mr. John Hibbard, Mr. Andrew Heath, Mr. Brennan Roney, and Ms. Supriya Kamatkar. The authors would like to thank the NCHRP IDEA project advisor Dr. Paul Carlson for his valuable inputs. The authors would like to thank the support from the NCHRP panel and from Georgia DOT (Andrew Heath), FDOT Florida DOT (Bouzid Choubane), Mississippi DOT (Mark Thomas and Cindy Smith), and Nevada DOT (Anita Bush) for providing their support and input on this research project. The authors would also like to thank Mr. David Adams and Mr. Carlos Baker from the Office of Traffic Operations and Mr. Jonathan Peevy, Mr. Shane Giles, Mr. Parker Niebauer from District 1, and other District 1 staff for their support in the field data collection using AllGather. Finally, we would like to Mr. Jason Nelson from the National Center of Asphalt Technology (NCAT) for supporting us to use the test track for our validation tests. The authors would like to thank Mr. Jon Lindsay's thorough editing on this final report. Finally, the authors would like to thank the support from Georgia Tech team members, including Dr. Cibi Pranav, Mr. Ryan Salameh, and Mr. Ron Knezevich.

# REFERENCE


AASHTO. A Policy on Geometric Design of Highways and Streets-2011. American Association of State Highway and Transportation Officials, Washington D.C., 2011.

Ai, Chengbo, and Yichang James Tsai. "Hybrid Active Contour–Incorporated Sign Detection Algorithm." Journal of Computing in Civil Engineering 26, no. 1 (2011): 28-36.

Albin, R, V Brinkly, J Cheung, F Julian, C Satterfield, W Stein, E Donnell, et al. Low-Cost Treatments for Horizontal Curve Safety 2016. FHWA-SA-15-084. FHWA, US Department of Transportation (2016).

Alessandretti, Giancarlo, Alberto Broggi, and Pietro Cerri. "Vehicle and Guard Rail Detection Using Radar and Vision Data Fusion." IEEE Transactions on Intelligent Transportation Systems 8, no. 1 (2007): 95-105.

Bassani, Marco, Nives Grasso, Marco Piras, and Lorenzo Catani. Estimating the Available Sight Distance on Urban Roads by Integrating 3d Maps and Low-Cost Mobile Mapping Systems into a Gis Numerical Computing Environment. (2016).

Bauer, Karin M, and Douglas W Harwood. "Safety Effects of Horizontal Curve and Grade Combinations on Rural Two-Lane Highways." Transportation research record 2398, no. 1 (2013): 37-49.

Bonneson, J, M. Pratt, J. Miles, and P. Carlson. "Development of Guidelines for Establishing Effective Curve Advisory Speeds". FHWA/TX-07/0-5439 1. Texas Department of Transportation, Austin, Texas, 2007.

Carlson, Paul, Mark Burris, Kit Black, and Elisabeth Rose. "Comparison of Radius-Estimating Techniques for Horizontal Curves." Transportation Research Record: Journal of the Transportation Research Board 1918 (01/01/ 2005): 76-83. https://doi.org/10.3141/1918-10. http://dx.doi.org/10.3141/1918-10.

Carlson, Paul, and Jr. John Mason. "Relationships between Ball Bank Indicator Readings, Lateral Acceleration Rates, and Vehicular Body-Roll Rates." Transportation Research Record: Journal of the Transportation Research Board 1658 (1999): 34-42. https://doi.org/doi:10.3141/1658-05. http://trrjournalonline.trb.org/doi/abs/10.3141/1658-05.

Chatterjee, Anirban. "A Methodology for Quantifying and Improving Pavement Condition Estimation and Forecasting by Integrating Smartphone and 3d Laser Data." Ph.D., Georgia Institute of Technology, 2019.

Donnell, Eric T, Kristin Kersavage, and Lisa F Tierney. Self-Enforcing Roadways: A Guidance Report. United States. Federal Highway Administration (2018).

FHWA (2021). Horizontal Curve Safety. https://safety.fhwa.dot.gov/roadway_dept/countermeasures/horicurves/ Accessed April 30, 2021.

FHWA. (2007). “Methods for Maintaining Traffic Sign Retroreflectivity.” https://safety.fhwa.dot.gov/roadway_dept/night_visib/policy_guide/fhwahrt08026/chapter3.cfm

FHWA. (2010). “Maintenance of Signs and Sign Supports.” https://safety.fhwa.dot.gov/local_rural/training/fhwasa09025/

Garber, Nicholas J, and Lester A Hoel. "Traffic and Highway Engineering." The Wadsworth Group, Pacific Grove 224 (2002).

Garyfallidis, Eleftherios, Matthew Brett, Marta Morgado Correia, Guy B Williams, and Ian Nimmo-Smith. "Quickbundles, a Method for Tractography Simplification." Frontiers in neuroscience 6 (2012): 175.

Glennon, John C, Timothy R Neuman, and Jack E Leisch. Safety and Operational Considerations for Design of Rural Highway Curves. Leisch (Jack E.) and Associates, 1985.

Glennon, John C., and James R. Loumiet. "Measuring Roadway Curve Radius Using the Compass Method." (2003). http://www.crashforensics.com/papers.cfm?PaperID=17.

Hu, Zhaozheng, and Yichang Tsai. "Homography‐Based Vision Algorithm for Traffic Sign Attribute Computation." Computer‐Aided Civil and Infrastructure Engineering 24, no. 6 (2009): 385-400.

Hummer, Joseph E, William Rasdorf, Daniel J Findley, Charles V Zegeer, and Carl A Sundstrom. "Curve Collisions: Road and Collision Characteristics and Countermeasures." Journal of Transportation Safety & Security 2, no. 3 (2010): 203-20.

Jun, Jungwook, Randall Guensler, and Jennifer Ogle. "Smoothing Methods to Minimize Impact of Global Positioning System Random Error on Travel Distance, Speed, and Acceleration Profile Estimates." Transportation Research Record: Journal of the Transportation Research Board 1972 (2006): 141-50. https://doi.org/doi:10.3141/1972-19. http://trrjournalonline.trb.org/doi/abs/10.3141/1972-19.

Kasa, I. "A Circle Fitting Procedure and Its Error Analysis." IEEE Transactions on Instrumentation and Measurement IM-25, no. 1 (1976): 8-14. https://doi.org/10.1109/TIM.1976.6312298.

Ku, Harry H. "Notes on the Use of Propagation of Error Formulas." (1966).

Lim, Kwangyong, Yongwon Hong, Yeongwoo Choi, and Hyeran Byun. "Real-Time Traffic Sign Recognition Based on a General Purpose Gpu and Deep-Learning." PLoS one 12, no. 3 (2017): e0173317.

Liu, H., S. Nassar, and N. El-Sheimy. "Two-Filter Smoothing for Accurate Ins/Gps Land-Vehicle Navigation in Urban Centers." IEEE Transactions on Vehicular Technology 59, no. 9 (2010): 4256-67. https://doi.org/10.1109/TVT.2010.2070850.

Ma, Weiyin, and J. P. Kruth. "Parameterization of Randomly Measured Points for Least Squares Fitting of B-Spline Curves and Surfaces." Computer-Aided Design 27, no. 9 (1995/09/01

1995): 663-75. https://doi.org/http://dx.doi.org/10.1016/0010-4485(94)00018-9. http://www.sciencedirect.com/science/article/pii/0010448594000189.

Milstead, R., Qin, X., Katz, B., Bonneson, J. A., Pratt, M., Miles, J., & Carlson, P. J. (2011). Procedures for setting advisory speeds on curves (No. FHWA-SA-11-22). United States. Federal Highway Administration. Office of Safety.

Moyer, R.A., and D.B. Berry. "Marking Highway Curves with Safe Speed Indications." Highway Research Board Proceedings. Highway Research Board, National Research Council, Washington, D.C., 1940, pp. 399-428

Manual on Uniform Traffic Control Devices. Federal Highway Administration, U.S. Department of Transportation, Washington, D.C., 2009.

Poe, Christopher M, Joseph P Tarris, and JM Mason Jr. Relationship of Operating Speeds to Roadway Geometric Design Speeds. (1996).

Qian, Rongqiang, Bailing Zhang, Yong Yue, Zhao Wang, and Frans Coenen. "Robust Chinese Traffic Sign Detection and Recognition with Deep Convolutional Neural Network." Paper presented at the 2015 11th International Conference on Natural Computation (ICNC), 2015.

"Imu Noise Model." 2019, https://github.com/ethz-asl/kalibr/wiki/IMU-Noise-Model.

Shih, Po-Cheng, Chi-Yi Tsai, and Chun-Fei Hsu. "An Efficient Automatic Traffic Sign Detection and Recognition Method for Smartphones." Paper presented at the 2017 10th International Congress on Image and Signal Processing, BioMedical Engineering and Informatics (CISP-BMEI), 2017.

Tsai, L-W, J-W Hsieh, C-H Chuang, Y-J Tseng, K-C Fan, and C-C Lee. "Road Sign Detection Using Eigen Colour." IET computer vision 2, no. 3 (2008): 164-77.

Tsai, Yichang James, and Chengbo Ai. "An Automated Superelevation Measurement Method for Horizontal Curve Safety Assessment Using a Low-Cost Mobile Device." Paper, 2016.

Tsai, Yichang James, and Zhaohua Wang. Validating Change of Sign and Pavement Conditions and Evaluating Sign Retroreflectivity Condition Assessment on Georgia's Interstate Highways Using 3d Sensing Technology. Georgia. Department of Transportation. Office of Performance-Based … (2019).

Tsai, Yichang, Pilho Kim, and Zhaohua Wang. "Generalized Traffic Sign Detection Model for Developing a Sign Inventory." Journal of Computing in Civil Engineering 23, no. 5 (2009): 266-76.

Tsai, Yichang, Qiang Yang, and Yiching Wu. "Use of Light Detection and Ranging Data to Identify and Quantify Intersection Obstruction and Its Severity." Transportation Research Record: Journal of the Transportation Research Board 2241 (2011): 99-108. https://doi.org/doi:10.3141/2241-11. http://trrjournalonline.trb.org/doi/abs/10.3141/2241-11.

Vedaldi, Andrea, Hailin Jin, Paolo Favaro, and Stefano Soatto. "Kalmansac: Robust Filtering by Consensus." Paper presented at the Tenth IEEE International Conference on Computer Vision (ICCV'05) Volume 1, 2005.

Wang, Zhaohua, and Yichang James Tsai. Exploration of Using Gdot's Existing Videolog Images and Pavement Surface Imaging Data to Support Statewide Maintenance Practices. Georgia. Dept. of Transportation. Office of Research (2016).

Zeng, Yujun, Xin Xu, Dayong Shen, Yuqiang Fang, and Zhipeng Xiao. "Traffic Sign Recognition Using Kernel Extreme Learning Machines with Deep Perceptual Features." IEEE Transactions on Intelligent Transportation Systems 18, no. 6 (2016): 1647-53.